University of Echahid Hamma Lakhdar – El Oued

Faculty of Technology

Department of Electrical Engineering

MASTER'S THESIS

Submitted in partial fulfillment of the requirements
for the degree of

Academic Master's Degree

Specialization: Electrical Control Engineering

Presentedby:

Bettahar Aymen

Ahmahma Mohammad Rami

Title:

Advanced Performance Optimization of PEMFC Systems Using Conventional, Intelligent, and Hybrid MPPT Control Strategies

Dr: Sarhoud Hisham	**President**
Dr: Al-Toumi Jaafar	**Examiner**
Dr:Chaouki Ilyes	**Thesis Suprvisor**

2025/2026

Dedication

I dedicate this work to my beloved parents,

whose endless love, prayers, sacrifices, and support have guided me throughout my life.

Their patience and encouragement have always been my source of strength and motivation.

To my dear brothers and sisters,

thank you for your kindness, support, and the joyful moments we shared during this journey.

To my family,

This achievement would not have been possible without your trust and belief in me.

Acknowledgments

First and foremost, I would like to express my deepest gratitude to my supervisor, Dr. Ilyas Chouki, for his valuable guidance, continuous support, patience, and encouragement throughout the preparation of this work. His advice and academic assistance were of great importance in completing this project.

I would also like to sincerely thank all the professors of Electrical Engineering and the Faculty of Technology for their efforts, dedication, and the knowledge they shared with us during our academic journey. We shared unforgettable moments, both joyful and difficult, and even the hard times were unintentional and part of the learning experience that helped us grow stronger and wiser.

My sincere appreciation also goes to the residence staff and workers for their efforts, kindness, and the services they provided throughout the years of study.

Finally, I extend my heartfelt thanks to everyone who supported me, encouraged me, and stood by my side during this journey.

Abstract

The growing demand for clean and sustainable energy systems has increased the interest in Proton Exchange Membrane Fuel Cells (PEMFCs) due to their high efficiency, low operating temperature, and environmentally friendly operation. The performance of PEMFC systems, however, strongly depends on efficient power management and suitable control strategies capable of ensuring operation at the Maximum Power Point (MPP) under varying operating conditions.

This work focuses on the modeling, simulation, and control of a PEMFC system associated with a hybrid Maximum Power Point Tracking (MPPT) strategy developed under the MATLAB/Simulink environment. The proposed system consists of a PEMFC stack, a DC-DC Boost converter, a PWM generation block, and an MPPT controller combining the conventional Perturb and Observe (P&O) algorithm with an Artificial Neural Network (ANN)-based intelligent approach.

A mathematical formulation of the PEMFC was first developed using a hybrid model integrating both stationary and dynamic behaviors. Amphlett's semi-empirical model was adopted to accurately represent the voltage characteristics of the fuel cell while considering activation, ohmic, and concentration losses. Different MPPT techniques were then analyzed, including conventional and intelligent approaches such as P&O, ANN, and Fuzzy Logic methods.

The proposed hybrid P&O–ANN controller was designed to improve tracking accuracy, reduce oscillations around the Maximum Power Point, and enhance the dynamic response of the system. Simulation results demonstrated that the hybrid approach provides better performance compared to the conventional MPPT method in terms of response speed, stability, and energy extraction efficiency. Furthermore, the integration of the Boost converter ensured efficient power transfer and stable output voltage characteristics.

The obtained results confirm the effectiveness of the proposed hybrid MPPT strategy for improving the overall performance of PEMFC energy systems. This

work also highlights the potential of artificial intelligence techniques in the development of advanced and efficient renewable energy control systems.

Keywords:

MPPT-PEMFC systems – Artificial intelligence technologies – Renewable energy

الملخص

أدى الطلب المتزايد على أنظمة الطاقة النظيفة والمستدامة إلى زيادة الاهتمام بخلايا الوقود ذات غشاء تبادل ، البروتونات (PEMFC) وذلك بفضل كفاءتها العالية، وانخفاض درجة حرارة تشغيلها، وطبيعتها الصديقة للبيئة. ومع ذلك، فإن أداء أنظمة في PEMFC يعتمد بشكل كبير على الإدارة الفعالة للطاقة واستراتيجيات التحكم المناسبة القادرة على ضمان التشغيل عند نقطة القدرة العظمي متغيرة (MPP) ظل ظروف تشغيل

يركز هذا العمل على نمذجة ومحاكاة والتحكم في نظام ، تم PEMFC مرتبط باستراتيجية هجينة لتتبع نقطة القدرة العظمي ، ومحول تيار Maximum Power Point Tracking - MPPT) تطويرها ضمن بيئة ، ووحدة MATLAB/Simulink MPPT ويتكون النظام المقترح من مكدس PEMFC مستمر إلى تيار - (مستمر من نوع ونهج ذكي (Boost DC-DC Boost Converter 0) ، وكتلة توليد PWM تحكم تجمع بين خوارزمية الاضطراب والملاحظة التقليدية .قائم على الشبكات Perturb and Observe Artificial Neural Networks - ANN(العصبية الاصطناعية

تم أولاً تطوير صياغة رياضية لنظام لتمثيل PEMFC باستخدام نموذج هجين يدمج بين السلوكيات الثابتة والديناميكية. وقد تم اعتماد النموذج شبه التجريبي لـ الوقود Amphlett خصائص الجهد الكهربائي لخلية P&O بدقة، مع الأخذ بعين الاعتبار خسائر التنشيط والخسائر الأومية وخسائر التركيز كما تم تحليل تقنيات مختلفة لتتبع نقطة القدرة العظمي (MPPT) ، بما في ذلك الأساليب التقليدية والذكية مثل خوارزمية والشبكات العصبية الاصطناعية (ANN) ، والمنطق الضبابي (Fuzzy Logic).

تم تصميم المتحكم الهجين P&O ANN بهدف تحسين دقة التتبع، وتقليل التذبذبات حول نقطة المقترحالقدرة العظمى، وتعزيز الاستجابة الديناميكية للنظام. وأظهرت نتائج المحاكاة أن النهج الهجين يوفر أفضل مقارنة MPPT أداة التقليدية من حيث سرعة الاستجابة، والاستقرار، وكفاءة استخراج الطاقة علاوة على ذلك، ساهم Boost بطريقة في ضمان نقل فعال للطاقة والحفاظ على خصائص مستقرة لجهد دمج محول الخرج

تؤكد النتائج المتحصل عليها فعالية استراتيجية MPPT الهجينة المقترحة في تحسين الأداء العام الأنظمة الطاقة المعتمدة على PEMFC كما يبرز هذا العمل الإمكانات الواعدة لتقنيات الذكاء الاصطناعي في تطوير أنظمة تحكم متقدمة وفعالة لمصادر الطاقة المتجددة

الكلمات المفتاحية :.تقنيات الذكاء الاصطناعي – الطاقة المتجددة – MPPT- PEMFC أنظمة

Résumé

La demande croissante en systèmes énergétiques propres et durables a suscité un intérêt accru pour les piles à combustible à membrane échangeuse de protons (PEMFC) en raison de leur rendement élevé, de leur faible température de fonctionnement et de leur caractère respectueux de l'environnement. Cependant, les performances des systèmes PEMFC dépendent fortement d'une gestion efficace de l'énergie et de stratégies de commande appropriées capables d'assurer un fonctionnement au point de puissance maximale (Maximum Power Point – MPP) sous des conditions de fonctionnement variables.

Ce travail porte sur la modélisation, la simulation et la commande d'un système PEMFC associé à une stratégie hybride de suivi du point de puissance maximale (Maximum Power Point Tracking – MPPT), développée sous l'environnement MATLAB/Simulink. Le système proposé se compose d'un empilement PEMFC, d'un convertisseur DC-DC Boost, d'un bloc de génération PWM et d'un contrôleur MPPT combinant l'algorithme conventionnel Perturb and Observe (P&O) avec une approche intelligente basée sur les réseaux de neurones artificiels (ANN).

Une formulation mathématique de la PEMFC a d'abord été développée à l'aide d'un modèle hybride intégrant à la fois les comportements stationnaires et dynamiques. Le modèle semi-empirique d'Amphlett a été adopté afin de représenter avec précision les caractéristiques de tension de la pile à combustible tout en prenant en compte les pertes d'activation, ohmiques et de concentration. Différentes techniques MPPT ont ensuite été analysées, incluant des approches conventionnelles et intelligentes telles que P&O, les réseaux de neurones artificiels (ANN) et la logique floue.

Le contrôleur hybride proposé P&O–ANN a été conçu pour améliorer la précision du suivi, réduire les oscillations autour du point de puissance maximale et renforcer la réponse dynamique du système. Les résultats de simulation ont démontré que l'approche hybride offre de meilleures performances par rapport à la méthode MPPT conventionnelle en termes de rapidité de réponse, de stabilité et d'efficacité d'extraction énergétique. En outre, l'intégration du convertisseur Boost a assuré un transfert efficace de puissance ainsi qu'une tension de sortie stable.

Mots-clés

Systèmes MPPT-PEMFC – Technologies d'intelligence artificielle – Énergies renouvelables

Les résultats obtenus confirment l'efficacité de la stratégie hybride MPPT proposée pour améliorer les performances globales des systèmes énergétiques à PEMFC. Ce travail met également en évidence le potentiel des techniques d'intelligence artificielle dans le développement de systèmes avancés et performants de commande des énergies renouvelables.

Contents

General Introduction 1

Chapter I: Proton Exchange Membrane Fuel Cell 4

Introduction 4

1.1Definition: 4

1.2 Working Principle. 6

Conclusion: 8

Chapter II: Mathematical Formulation of PEMFCs' Model: 9

Introduction 9

2.1 Hybrid Mathematical Model: 9

2.1.1 The Model Under Analysis: 9

1.1.2 Amphlett's Semi-Empirical Model of PEMFC: 12

Conclusion 16

Chapter III:Maximum Power Point Tracking Algorithm: 18

Introduction 18

3.1 Fundamentals Maximum Power Point Tracking Algorithm: 18

3.2Development of Different PowerPoint Tracking Methods: 20

3.2.1P&O Algorithm. 21

3.2.2Artificial Intelligence: 22

3.2.2.1Functional Network-Based MPPT Controller:..... 23

3.2.2.2Fuzzy Logic Control:..... 25

3.3 Hybrid ANN–P&O Based Maximum Power Point Tracking for PEM Fuel Cell Systems :..... 27

Conclusion: 28

..... 17

ChapterVI:Simultion and Performance Analysis of Hybrid MPPT Techniques For PEMFC Systems:..... 29

Introduction:..... 29

4.1. PEMFC Simulation Model:..... 29

4.2. Modeling of the Boost DC-DC Converter : 33

4.3 Hybrid MPPT Control Block : 35

4.3.1 Conventional P&O MPPT Algorithm: 35

4.3.2 ANN – Based MPPT Controller:..... 42

4.4 Design and Simulation of Hybrid Classical and ANN – Based MPPT Controller:..... 52

Conclusion: 59

General Conclusion..... 58

References:..... 60

List of Figures

Figure1.1:Schematic of A Fuel Cell……7

Figure2.1: The PEMFC Model 10

Figure 2.2 : Detailed PEMFC Dynamic Model……. 12

Figure 2.3 : Simplified PEMFC Dynamic Model,,,,,,,,,,..... 13

Figure 2.4 : Equivalent Circuit Per Cell 13

Figure 2.5 Fuel Cell Losses 14

Figure 3.1:Diagram of The MPPT Control System Of PEMFC 18

Figure 3.2: Fuel Cell Power-Current And Voltage-Current Characteristics ……..... 19

Figure 3.3 : Flowchart of The P&O Algorithm For PEMFC 20

Figure 3.4 : RBFN Working Process For PEMFC-Based Power Supply System 23

Figure 3.5 : Fuzzy Current Control Diagram…….. 25

Figure 3.7 : Fuzzy Logic Membership..... 26

Figure 4.1 : Simulink Model Of The PEMFC System..... 28

Figure 4.2 : Step Block Parameter Configuration In Simulink…..... 29

Figure 4.3 : Step 1 Block Parameter Configuration In Simulink 29

Figure 4.4 : Simulation Of A DC-DC Boost Converter Using MATLAB/Simulink 31

Figure 4.6 : PWM Switching Waveform Of The DC-DC Boost Converter ……..……..... 33

Figure 4.7 : Simulink Implementation Of The Conventional P&O MPPT Controller..... 36

Figure 4.8:Voltage FC(Source Et Load) Signal…….36

Figure 4.9: Current FC (Source Et Load) Signal……37

Figure 4.10: Duty Cycle Signal……...……38

Figure 4.11:Power (Fc-Source Et Load) Signal……..39

Figure 4.12 : Simulink Implementation Of The MPPT..... 46

Figure 4.13 : Simulink Implementation Of The Conventional ANN MPPT Controller..... 47

Figure 4.14:Voltage Fc (Source Et Load)Signel…….....47

Figure 4.15:Current Fc (Source Et Load)Signal…….....48

Figure 4.16:Duty Cycle Signal……48

Figure 4.17:Power(Fc-Source Et Load)Signal……49

Figure 4.18: Proposed Hybrid MPPT Control Scheme Based on P&O and ANN For a PEMFC.....…… …….…….……52

Figure 4 .19:MATLAB / Simulink Implementation of The Hybrid P&O - ANN MPPT Controller For PEMFC System…….…….….53

Figure 4.20: Voltage Fc (Source Et Load)Signal……..……..……54

Figure 4.21:Courrent Fc(Source Et Load)Signal……54

Figure 4.22:Duty Cycle Signal……..…….55

Figure 4.23:Power(Fc -Source Et Load)Signal……...…55

List of Tables

Table 3.6 : Fuzzy Logic Rules 25

Table 4.5 : DC-DC Boost Converter Parameters 31

Table 4 .24 : Comparison Between Classical, Intelligent, and Hybrid MPPT Control Strategies for PEMFC systems.....57

Nomenclature and Abbreviations

1. Abbreviations

AC	Alternating Current
ANN	Artificial Neural Network
CO	Carbon Monoxide
CO_2	Carbon Dioxide

DC	Direct Current
DFT	Density Functional Theory
EV	Electric Vehicle
FC	Fuel Cell
FC-PCC	Fuzzy-Predictive Current Control
GDL	Gas Diffusion Layer
HOR	Hydrogen Oxidation Reaction
HT-PEMFC	High-Temperature Proton Exchange Membrane Fuel Cell
IT	Intermediate Temperature
IT-PEMFC	Intermediate-Temperature Proton Exchange Membrane Fuel Cell
LT-PEMFC	Low-Temperature Proton Exchange Membrane Fuel Cell
MEA	Membrane Electrode Assembly
MPPT	Maximum Power Point Tracking
MOSFET	Metal-Oxide-Semiconductor Field-Effect Transistor
ORR	Oxygen Reduction Reaction
P&O	Perturb and Observe
PBIs	Polybenzimidazoles
PEM	Proton Exchange Membrane
PEMFC	Proton Exchange Membrane Fuel Cell

PWM	Pulse Width Modulation
RBF	Radial Basis Function
RMSE	Root Mean Square Error
R^2	Coefficient of Determination
SOFC	Solid Oxide Fuel Cell
nftool	Neural Fitting Tool (MATLAB)
Simulink	Simulation and Link

2Nomenclature (Symbols)

Symbol	Description	Unit
2e−	Two electrons	–
2H+	Two protons	–
C	Capacitance	F
Cdca	Double-layer capacitance (anode & cathode)	F
D	Duty cycle	–
E_0	Ideal open circuit voltage	V
H2	Hydrogen	–
H2O	Water	–
IFC / Ifc	Fuel cell current	A
JOX	Exchange current density	A/cm^2
JLX	Limiting current density	A/cm^2
LL	Inductance	H
O2	Oxygen	–
Rm	Membrane resistance	$\Omega \cdot cm^2$

Symbol	Description	Unit
Rta	Transfer resistance (anode & cathode)	Ω
rm	Internal resistance	Ω
rtx	Transfer resistance	Ω
V0	Initial voltage	V
VFC / Vfc	Fuel cell voltage	V
VMP	Voltage at maximum power point	V
Vsta	Stack voltage	V
Vi	Input voltage	V
WOa, WRa	Warburg impedance (anode)	Ω
WOc, WRc	Warburg impedance (cathode)	Ω
bx	Tafel slope / Charge transfer coefficient	V^{-1}
k	Sampling instant	–
ηact	Activation overpotential	V
ηconc	Concentration overpotential	V
ηohm	Ohmic overpotential	V
ΔIref	Change in reference current	A
Δe(k) / DE	Change in error	–
e(k)	Error at sample kk	
C	Capacitance	F
D	Duty cycle	–
DU	Duty cycle variation	–
Iout	Output current	A
L	Inductance	H
Req	Equivalent load resistance	Ω
RL	Actual load resistance	Ω
Vin	Input voltage	V
VMPP	Voltage at maximum power point	V
Vout	Output voltage	V
Vsta	Stack terminal voltage	V
α	Charge transfer coefficient	-

General Introduction

General Introduction

The global energy transition is now considered a strategic priority. Indeed, the gradual depletion of fossil resources, combined with the increasingly visible effects of climate change, is pushing countries to rethink their energy models. Furthermore, energy demand continues to rise, which accentuates the risks linked to the scarcity of these resources and global warming. In this context, it becomes essential to direct efforts towards a more sustainable and environmentally friendly energy system .[1]

Thus, the energy sector is decisively reorienting itself towards a clean and sustainable production system. While the renewable energy sector, including solar and wind, is experiencing rapid growth, this rise of renewable sources requires a return to highly reliable energy vectors capable of storing and releasing energy when production conditions are not ideal. It is in this context that hydrogen emerges as a promising solution for the future, and fuel cells are today the most advanced electrochemical conversion technology for transforming hydrogen into electricity with high efficiency and almost zero carbon emissions .[2]

Of the various technologies available, the proton exchange membrane fuel cell (PEMFC) is of particular interest at both industrial and academic levels. It is characterized by its relatively low operating temperature, high power density, compact design, and fast start-up capability. These features make it an ideal candidate for a wide range of applications, from stationary micro cogeneration units to automotive propulsion, as well as embedded systems and microgrids .The choice of proton exchange membrane fuel cell (PEMFC) technology is motivated by its promising performance, including low weight, high robustness, a solid electrolyte, rapid start-up, and a wide power range .[3]

Efficient power extraction from Proton Exchange Membrane Fuel Cell (PEMFC), The operating point is continuously adjusted to reach the maximum power under varying working conditions using Maximum Power Point Tracking, or MPPT, techniques. In this paper, different methods for maximising the output power

of a fuel cell are presented. First, the classical Perturb and Observe (P&O) method is discussed. This technique is widely used due to its simple structure and easy implementation; it is affected by the steady state oscillations and limited response speed when the operating conditions are changing rapidly.[4]

To overcome these drawbacks, advanced intelligent control techniques such as neural network-based regulators and fuzzy logic controllers are investigated. Compared with traditional methods, these methods have faster tracking capability, higher accuracy, and better system stability. The main target of this work is to suggest an advanced hybrid MPPT technique to ensure a dependable, steady, and efficient power extraction from the PEMFC system under various operating conditions.[5]

This research aims to improve the performance of proton exchange membrane fuel cell systems by developing a hybrid MPPT control strategy based on artificial intelligence, in order to optimize integrated energy management and maximize the extracted power while reducing losses and enhancing the dynamic stability of the system.

In addition to a general introduction and a general conclusion, which summarize our study, the present work is divided into four chapters organized as follows:

The first chapter provides an overview of PEM fuel cell technology and its main characteristics. It explains the operating principle, focusing on the electrochemical reactions at the anode and cathode. The role of the proton exchange membrane in proton transport is also highlighted. Overall, it establishes the theoretical foundation for hydrogen-to-electricity conversion and prepares for the following chapters.

Chapter 2 presents the mathematical modeling of the PEMFC for numerical simulation. It is based on the semi-empirical Amphlett model to describe the polarization curve. The model includes activation, ohmic, and concentration losses to simulate fuel cell performance in MATLAB under different conditions accurately.

Chapter 3 studies Maximum Power Point Tracking (MPPT) methods for extracting maximum power from the PEMFC. It begins with the conventional P&O algorithm and discusses its limitations, including oscillations and slow response. It then introduces artificial intelligence techniques such as neural networks and fuzzy logic to improve performance. The objective is to develop an optimized hybrid MPPT strategy for efficient and stable power extraction.

Chapter 4 presents the implementation of the developed models and MPPT algorithms using MATLAB/Simulink. A complete system including the PEM fuel cell, DC-DC converter, and control strategies is simulated. The performance of different MPPT methods is evaluated under various operating conditions. The results show that the proposed hybrid approach offers better speed, accuracy, and efficiency compared to conventional techniques.

We conclude this study by summarizing the achievements accomplished and highlighting their contributions to the field of renewable energy. We also present new research perspectives, such as the integration of deep learning techniques or the development of intelligent systems capable of adapting to more complex environments.

By integrating both theory and practice, this work aims to promote innovation toward sustainable and efficient energy systems.

Chapter Ⅰ:

Proton Exchange Membrane Fuel Cell

Chapter Ⅰ: Proton Exchange Membrane Fuel Cell

Introduction

The transition to clean and sustainable energy sources is essential and inevitable, in view of the problems posed by climate change and the slow depletion of fossil fuels. In such a context, the electrochemical energy conversion technologies are gaining popularity. [6]

Among these technologies, the proton exchange membrane fuel cell (PEMFC) is one of the most developed and studied systems worldwide. It was first developed in the 1960's in the American space program and has advanced significantly due to advances in proton-conducting polymer membranes, achieving high power densities with zero emissions at the point of use .[7]

The PEMFC operates using hydrogen as a fuel and oxygen from the air as the oxidant to produce electricity, heat, and pure water directly. Its relatively low operating temperature, typically between 60 °C and 80 °C, along with its fast start-up and high power density, makes it a strong candidate for both transportation applications and stationary power generation systems .[8]

1.1Definition:

In a typical Proton Exchange Membrane Fuel Cell (PEMFC), the polymer electrolyte membrane is critical for proton conductivity, enabling transport of protons from the anode to the cathode. Among various fuel cell membrane types, perfluorosulfonic acid polymers such as Nafion are widely used due to their high conductivity and robust chemical and mechanical properties. These membranes operate below 90°C under high relative humidity. Developed by DuPont in the late 1960 Nafion remains the leading low-temperature PEM membrane. However , Nafion faces challenges for low-temperature PEMFCs (LT-PEMFCs) due to expensive production and decreased proton conductivity above 90°C ,triggered by loss of ion-exchange groups starting at 130°C. These limitations have driven the

development of intermediate-temperature PEMFCs (IT-PEMFCs) and high-temperature PEMFCs (HT-PEMFCs), operating between 100–150°C and 120–200°C, respectively, under dry conditions, which are the focus of this review.

At moderate and high temperatures, electrode poisoning by CO and CO_2 reduces catalytic activity. Nonetheless, IT-PEMFCs and HT-PEMFCs benefit from faster electrode kinetics, simpler thermal and water management, less dependence on cooling systems, greater recoverable heat, and lower membrane-electrode assembly (MEA) costs compared to Nafion-based LT-PEMFCs. The high CO tolerance of anode catalysts allows direct hydrogen usage from simple methanol reformers, easing or eliminating the need for selective oxidants or CO separators, thus reducing fuel cell size and enhancing performance, responsiveness ,reliability, and lowering maintenance and operation costs.

Considerable research has focused on optimizing IT-PEMs and HT-PEMs, especially using sulfonated polyether ether ketone (SPEEK) and polybenzimidazoles (PBIs), which show promise for moderate and high-temperature

Growing global energy demand and environmental concerns emphasize the importance of clean, renewable energy sources to replace fossil fuels, whose combustion increases atmospheric CO_2 and contributes to global warming and climate change. Electrochemical catalytic conversion of renewable electricity and carbon oxides into chemicals and fuels is gaining attention as a way to mitigate the energy crisis through a closed carbon cycle, enabling storage and reconversion of chemical fuels like hydrogen into electricity via fuel cells.

PEMFCs are increasingly seen as promising clean energy sources for industrial applications, portable devices, and transportation .Electrocatalysts are vital for achieving a sustainable hydrogen-based energy cycle. The Sabatier principle and density functional theory (DFT) are employed to assess the reactivity and catalytic activity of new electrode materials for fuel cell applications.

There is a significant effort to develop low-cost, efficient electrocatalysts for electrolyzers and fuel cells using abundant ,environmentally friendly, and stable

materials. New nanomaterials, including metals, metal oxides, and non-metals, are synthesized with controlled shape, size, composition, architecture ,and micro-nanostructures to optimize catalytic properties. Alloying or doping catalysts can modify surface states, changing intermediate binding energies during reactions.

This thesis aims to provide an overview of recent experimental synthesis methods for H_2/O_2 PEMFC components and to evaluate material performance, thereby advancing the field. A key challenge in low-temperature fuel cells is overcoming the slow oxygen reduction reaction (ORR), which is at least four orders of magnitude slower than the hydrogen oxidation reaction (HOR). This necessitates catalytic materials with high activity, stability, durability, and selectivity at the cathode to accelerate oxygen reduction in energy conversion devices. The fundamental electrochemical reactions occurring at both electrodes of the PEMFC membrane-electrode assembly (MEA) are detailed in the literature.[9]

1.2 Working Principle.

The demand for sustainable energy has increased interest in fuel cells more than ever in the modern era, illustrating the PEMFC's operating principle. PEMFC's functionality relies on the transport of H_2 in the form of two protons[2H+] and two electrons [2e-] from the anode to the cathode. The protons are transported through a proton exchange membrane electrolyte, releasing electrons through an external circuit.

$$H_2 \rightarrow 2H+ + 2e- \quad (1)$$

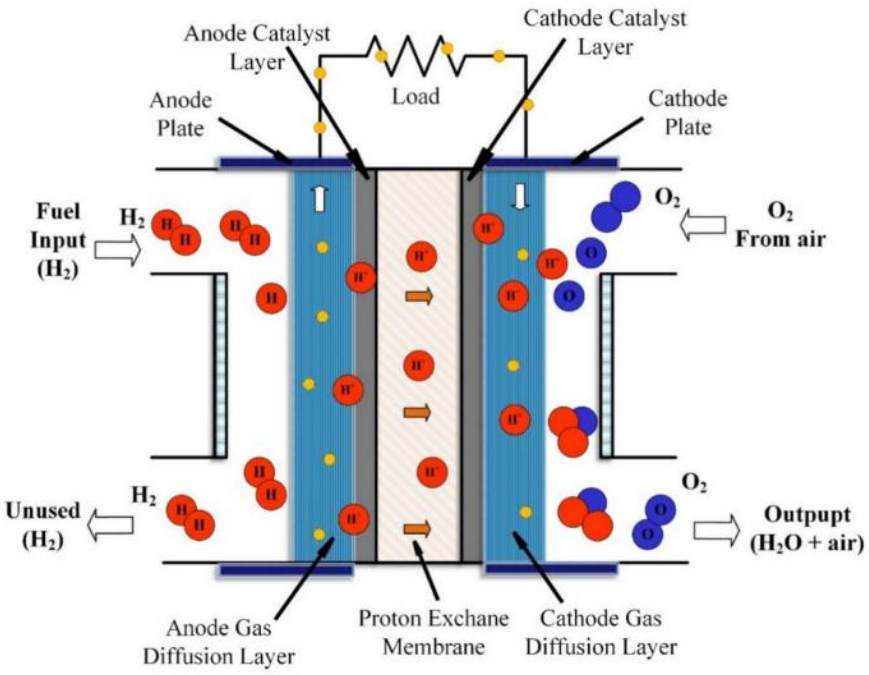

Figure 1.1Schematic of a Fuel Cell.[10]

When H+ ions migrate to the acidic electrolyte, the electrons are compelled to move toward the cathode, thus electricity flows in the external circuit. Water is created at the cathode side by the interaction of oxygen, hydrogen ions, and electrons with a stream of external gas flow.

$$O_2 + 4H+ + 4e- \rightarrow 2H_2O \qquad (2)$$

The two main electrochemical processes may be combined to give:

$$2H_2 + O2 \rightarrow 2H_2O \qquad (3)$$

The hydrogen and oxygen/air enter the PEMFC through their respective flow channels and spread through the gas diffusion layer (GDL). The hydrogen gas releases H+ ions at the catalyst site of the anode, which are allowed to pass through the proton exchange membrane electrolyte to the cathode domain. The electrons released during the formation of protons in hydrogen are directed into the external circuit, producing an electric current. The schematic of the PEMFC is shown in Fig.1.1. The protons available at the cathode side combine with the electrons from

the external circuit and O_2 to form water. The product, water, is then expelled from the fuel cell exhaust via the cathode flow channel. The efficiency of a PEMFC is greatly dependent on the conductivity of the proton through the membrane electrolyte. The membrane should be optimally hydrated to enable efficient proton transfer, whilst not over-saturating the fuel cell; thus, water management of the electrolyte becomes crucial to maximising performance.[11]

Conclusion:

The Proton Exchange Membrane Fuel Cell (PEMFC) is a highly efficient electrochemical system for direct energy conversion. By analyzing its operating principles—specifically the redox reactions at the electrodes and the selective transport through the membrane it becomes evident that while the system offers significant advantages like high power density and zero emissions, its stability is strictly governed by operating conditions. These fundamental insights provide the necessary theoretical framework for the mathematical modeling and governing equations that will be developed in the subsequent chapter to describe the system's dynamic behavior."

Chapter II:

Mathematical Formulation of PEMFC Model

Chapter II: Mathematical Formulation of PEMFCs' Model:

Introduction

With the increasing interest in clean energy technologies, Proton Exchange Membrane Fuel Cells (PEMFCs) have become an important part of hybrid electrical energy management systems. Because of their high efficiency, low operating temperature, and zero harmful emissions, PEMFCs have been extensively investigated for applications in such configurations. For accurate analysis and optimisation of these systems, a precise mathematical model of the PEMFC is necessary. Among the existing modelling approaches, the Amphlett's semi-empirical model is widely used in the literature. [12]

2.1 Hybrid Mathematical Model:

Modeling the Proton Exchange Membrane Fuel Cell (PEMFC) is a crucial step for accurately analyzing the system's behavior under various operating conditions ,especially in control and energy management applications. Because these systems are nonlinear and complex, relying on a single model to capture all physical and dynamic phenomena is not feasible. Instead ,a hybrid modeling approach was used, combining two models from reputable scientific studies to balance physical accuracy and dynamic behavior representation.

2.1.1 The Model Under Analysis:

The model considered in this paper captures both stationary and dynamic behaviors, allowing simulation of the PEMFC stack under any operating condition. The outputs of the static and dynamic parts are run separately and then superimposed to provide the total stack voltage output. The input current is first split into its DC

and AC components. The static analytical model receives the DC as input and produces the DC voltage as output. The analytical expression for the static part represents the output DC voltage by subtracting the internal ohmic losses from the ideal potential (E0). (ηohmic) and chemical reactions (activation losses, ηact, and concentration losses, ηconc). This theoretical expression is derived from the Nernst law.

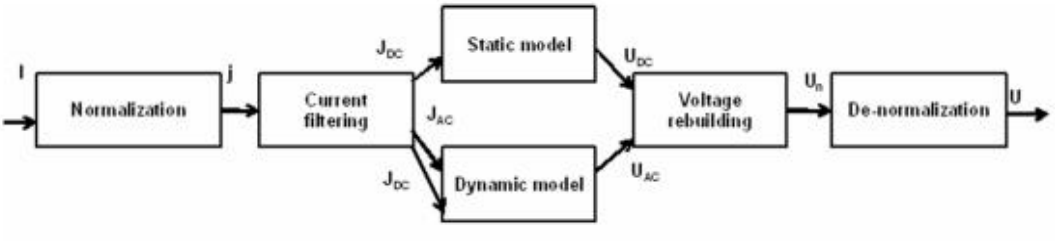

Figure 2.1The PEMFC Model.

$$V_{cell} = E_0 - \eta_{cathode} - \eta_{anode} - \eta_{ohmic} \quad (4)$$

Where:

$$\eta_{ohmic} = R_m \cdot I \quad (5)$$

$$\eta_{cathode} = \frac{1}{b_c} a\sinh\left(\frac{J_{DC}}{2J_{OC}\cdot\left(1-\frac{J_{DC}}{J_{LC}}\right)}\right) \quad (6)$$

$$\eta_{anode} = \frac{1}{b_a} a\sinh\left(\frac{J_{DC}}{2J_{OA}\cdot\left(1-\frac{J_{DC}}{J_{LC}}\right)}\right) \quad (7)$$

The parameters are :

- **E0 [V]** represents the theoretical ideal potential in standard conditions, derived from chemical reactions.

- **Rm [cm2]** is the internal ohmic resistance of the membrane, mostly due to the electrolyte ionic resistance, but also to metallic contacts.
- **bx [V1]** is theTafel slope or electrode charge transfer coefficient, describing the reaction's kinetics.
- **JOX[A/cm2]** is the diffusion current either for the cathode or the anode.
- **JLX [A/cm2]** is the limiting current, i.e., the maximum current theoretically achievable ,depending on the reactants' diffusion velocity.

Experimental tests demonstrated that the limiting current at the anode is so high that its influence on the output voltage is negligible.

An alternative simplified analytic expression, not including distinctions between anode and cathode, can be considered; the result is an approximate model with a smaller number of parameters to be fitted:

$$U_{DC} = E_0 - R_m \cdot J_{DC} - \frac{1}{b}\ln\left(\frac{J_{DC}}{2J_O \cdot \left(1-\frac{J_{DC}}{J_L}\right)}\right) \quad (8)$$

The dynamic behavior of the PEMFCs' stack is described through an equivalent electrical circuit, depicted in Fig.2.2. It includes:

- The internal resistance ,**rm** ,accounts for the ionic membrane resistance and the ohmic contacts resistance .

- The transfer resistances ,**rtx** ,account for the ion transfer speed from the electrode into the electrolyte .

- The double-layer capacitances ,**cdcx** ,account for the charge accumulation at the electrode/electrolyte interface .

- Thewarburg impedances ,**wox wrx ,**accounting for diffusion phenomena, respectively for the oxidant and reductant species .

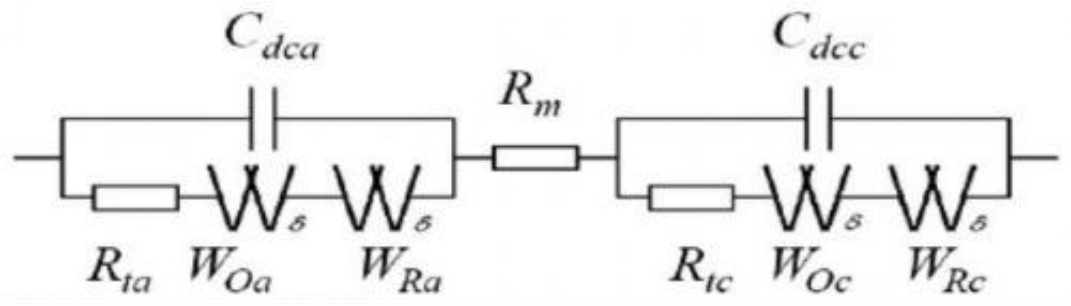

Fig2.2: Detailed PEMFC Dynamic Model

The Warburg impedance for the anode (**WOa**, **WRa**) is not so relevant and can be neglected, as well as the impedance due to the oxygen reduction reactions at the cathode (**WRc**). As a consequence, the model shown in Fig.2.3. has been used, so that the parameters involved in the parametric analysis are: **Rm**, **Rta**, **Rtc**, **Cdca**, **Cdcc**, **WOc.** [13]

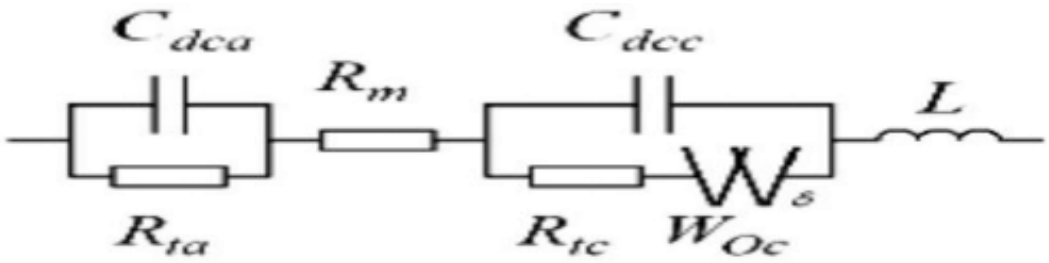

Fig2.3: Simplified PEMFC Dynamic Model.

1.1.2 Amphlett's Semi-Empirical Model of PEMFC:

As formerly stated, Amphlett's model is regarded as the most powerful method to simulate the dependency of the PEMFC's terminal voltage on the load current through various steady-state cases. In order to examine the PEMFC stack in operation, Mann and Amphlett's PEMFC model makes several simplifying assumptions. Here are a few of these presumptions: (I) The fuel and oxidant gas compositions are constant and precisely blended throughout the entire cell, (II) The

electrodes completely consume the fuel and oxidant, preventing any buildup inside the cell, (III) There is no gas mixing between the anode and cathode compart ments because the fuel and oxidant gases run parallel to the electrodes, and (IV) The porosity and thickness of the material do not change over time, (V) The fuel and oxidant gases' temperature, pressure, and humidity remainconstant across the entire cell, and (VI) the electrolyte is a perfect ion conductor with no limits on electronic conductivity or mass transfer.

Despite the aforementioned, Mann's model can be extended to describe the transient behavior as well. Amphlett supposes that the PEMFC's terminal voltage is subjected to three voltage decays, which are the activation, the ohmic, and the concentration voltage drops, as described in Fig2.4The next few statements are concise

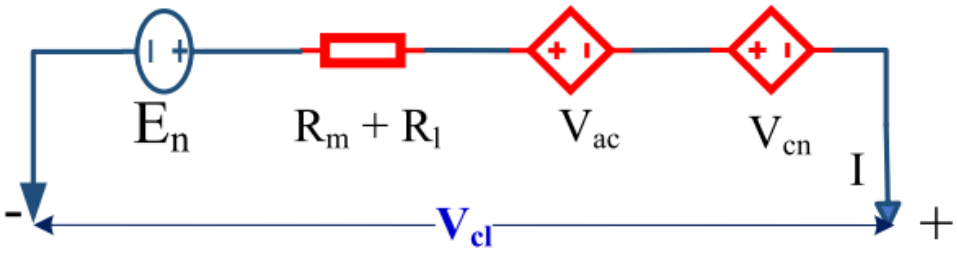

Fig 2.4: Equivalent Circuit Per Cell.

illustrate the model, as thoroughly described in the state-of-the-art. The terminal voltage per single cell, V_{cl} (V), is given by.

$$V_{cl} = E_n - V_{ac} - V_{oh} - V_{cn} \tag{9}$$

where ,

where, $\boldsymbol{E_n}$ is the Nernst open-circuit voltage per PEMFC in (V), $\boldsymbol{V_{ac}}$ is the activation over-potential in (V) as the startup chemical reactions are relatively slow, $\boldsymbol{V_{oh}}$ is the ohmic voltage loss due to the total resistance of the membrane and

external leads in (V) and $\boldsymbol{V_{cn}}$ is the concentration over-potential due to the high water content in the membrane at heavy loading in (V).

As earlier mentioned, to attain a high terminal voltage, N PEMFCs are connected in series, creating a PEMFC stack whose terminal voltage is $\boldsymbol{V_{st}}(V)$ and calculated by (2).[14]

$$V_{st} = N \cdot V_{cl} \tag{10}$$

The polarization curve of a fuel cell operating at 80°C. The curve features three distinct regions: activation losses, ohmic losses, and concentration losses. The nonlinear activation zone provides insights into the electrochemical processes within the cell. Ohmic losses typically occur in the membrane, while concentration losses result from changes in the concentration gradient within the cell Fig2.5.

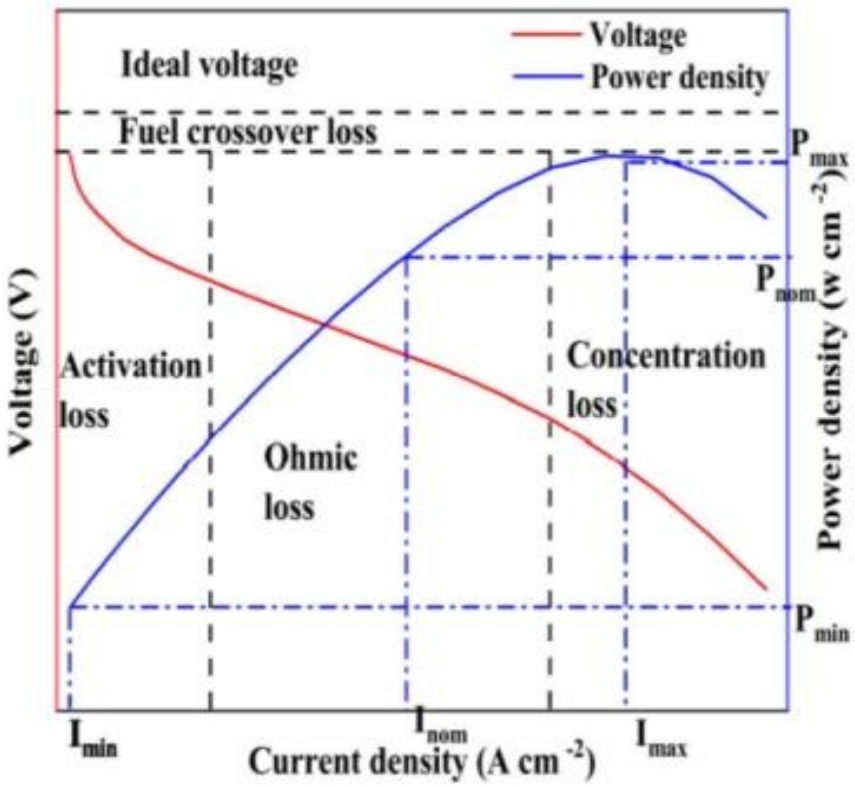

Fig.2.5 Fuel Cell Losses

Eq (3) considers the variation in temperature surrounding the cell. The open circuit voltage (**Ecel**) is given by:

$$E_{\text{cell}} = \begin{cases} 1229 - \frac{44.43}{zF}(T - 298.15) + \frac{rT}{zF}\ln\left(P_{\text{H}_2}\sqrt{P_{\text{O}_2}}\right) & \text{for } T \leq 273 \\ 1229 - \frac{44.43}{zF}(T - 298.15) + \frac{rT}{zF}\ln\left(\frac{P_{\text{H}_2}\sqrt{P_{\text{O}_2}}}{P_{\text{H}_2\text{O}}^{\text{Sat}}}\right) & \text{otherwise} \end{cases} \quad (11)$$

In these eqs, $\boldsymbol{r}, \boldsymbol{F}$, and $\mathbf{z}$ represent the ideal gas constant, Faraday constant, and number of moving electrons, respectively. The temperature of the cell is denoted by $\boldsymbol{T}$,while $\boldsymbol{P}_{\mathbf{H_2}}$and $\boldsymbol{P}_{\mathbf{O_2}}$represent the partial pressures of hydrogen and oxygen. The partial pressures are quantified in eq (12) and (13).

$$P_{\text{H}_2} = 0.5 \times \text{RH}_\text{a} \times P_{\text{H}_2\text{O}}^{\text{Sat}} \left(\left(\frac{\text{RH}_\text{a} \times P_{\text{H}_2\text{O}}^{\text{Sat}}}{P_a} \times \exp\left(\frac{1.635 \times i_{\text{cell}}/\text{A}}{T^{1.334}} \right) \right)^{-1} - 1 \right) \quad (12)$$

$$P_{\text{O}_2} = \text{RH}_\text{c} \times P_{\text{H}_2\text{O}}^{\text{Sat}} \left(\left(\frac{\text{RH}_\text{c} \times P_{\text{H}_2\text{O}}^{\text{Sat}}}{P_c} \times \exp\left(\frac{1.635 \times i_{\text{cell}}/\text{A}}{T^{1.334}} \right) \right)^{-1} - 1 \right) \quad (13)$$

Here, $\mathbf{RH}_{\boldsymbol{a}}$ and $\mathbf{RH}_{\boldsymbol{c}}$ denote the anodic and cathodic relative humidity, respectively. The pressures at the anode and cathode are $\boldsymbol{P}_{\boldsymbol{a}}$ and $\boldsymbol{P}_{\boldsymbol{c}}$, respectively. The cell area is A and the current is i_{cell}. The relationship between temperature $\boldsymbol{T}$ and the vapor saturation pressure of water $\boldsymbol{P}_{\mathbf{H_2O}}^{\mathbf{Sat}}$ is given by eq (14). Semi-empirical parameters $\boldsymbol{\delta_1}$, $\boldsymbol{\delta_2}$, $\boldsymbol{\delta_3}$, and $\boldsymbol{\delta_4}$ are used to calculate the activation losses, as shown in eq (15). The oxygen concentration $\mathbf{CO_2}$ is determined by eq (16), while the ohmic losses are calculated using eq (17).

$$\log_{10}\left(P_{\text{H}_2\text{O}}^{\text{Sat}}\right) = 2.95 \times 10^{-2}(T - 273.15) - 9.19 \times 10^{-5}(T - 273.15)^2 \quad (14)$$

$$V_{\text{act}} = -\left(\delta_1 + \delta_2 T + \delta_3 T \ln\left(C_{\text{O}_2}\right) + \delta_4 T \ln(i_{\text{fc}})\right) \quad (15)$$

$$C_{\text{O}_2} = \frac{P_{\text{O}_2}}{5.08 \times 10^6} \exp\left(\frac{498}{T}\right) \quad (16)$$

$$V_{\text{ohmic}} = i(R_m + R_c) \quad (17)$$

Electrical and ionic resistances are represented by $\boldsymbol{R_m}$ and $\boldsymbol{R_c}$. eq (18) calculates electronic resistance, and eq (19) determines the membrane parametric coefficient. Concentration polarization is mathematically expressed using eq (20).The maximum current density is $\boldsymbol{J_{max}}$, while $\boldsymbol{J}$ is the actual current density, and $\boldsymbol{B}$ is the parametric coefficient or diffusion parameter.[15]

$$R_m = \rho_m \left(\frac{l}{A}\right) \tag{18}$$

$$\rho_m = \frac{181.6\left[1+0.03\left(\frac{i}{A}\right)+0.062\left(\frac{T}{303}\right)^2\left(\frac{i}{A}\right)^{2.5}\right]}{\left[\gamma-0.634-3\left(\frac{i}{A}\right)\right]\times\exp\left(4.18\left(\frac{T-303}{T}\right)\right)} \tag{19}$$

$$V_{\text{conc}} = -B\ln\left(1-\frac{J}{J_{max}}\right) \tag{20}$$

Conclusion :

The mathematical formulation of the Proton Exchange Membrane Fuel Cell (PEMFC) was developed through a hybrid modeling approach that combines both stationary and dynamic behaviors of the system. This representation allows a more realistic description of the fuel cell performance under different operating conditions. The adopted model considers the main physical and electrochemical phenomena governing the fuel cell, ensuring an accurate representation of its output characteristics.

In particular, Amphlett's semi-empirical model was utilized to describe the voltage behavior of the PEMFC, taking into account the different voltage losses such as activation, ohmic, and concentration losses. This approach provides a good compromise between model simplicity and accuracy. The developed formulation constitutes a solid basis for system analysis and plays a key role in understanding

the fuel cell response, which is essential for the design and implementation of effective control strategies.

Chapter III:

Maximum Power Point Tracking Algorithm

Chapter III:Maximum Power Point Tracking Algorithm:

Introduction

The continuous pursuit of higher efficiency in hybrid electrical energy management systems has driven considerable research efforts toward the development and refinement of Maximum Power Point Tracking (MPPT) algorithms. Since PEMFCs exhibit a nonlinear power-voltage characteristic that varies with operating conditions such as temperature, pressure, and hydrogen flow rate, dedicated tracking strategies are required to ensure that the system consistently extracts them aximum available power from the fuel cells tack .[16] To address this challenge, several MPPT methods have been proposed and evaluated in the literature. Among the conventional approaches, the Perturb and Observe (P&O) algorithm remains one of the most frequently employed techniques, owing to its straightforward implementation and minimal parameter requirements. Nevertheless, this method presents notable limitations, particularly its tendency to oscillate around the maximum power point and its reduced effectiveness under dynamically changing load conditions. [17]

3.1 Fundamentals Maximum Power Point Tracking Algorithm:

The diagrammatic sketch of the MPPT control system of PEMFC with a boost converter, which is mainly composed of PEMFC, boost converter, MPPT controller, PWM generator, and external load resistance. Because the Boost converter has the advantages of simple structure, easy control, and voltage amplification, it is used in the system to improve the output voltage and as a regulator to realize the MPPT control scheme. The output of the PWM generator is a series of square waves with different duty cycles, which is used to control the ON and OFF of the Boost converter. The output duty

cycle of the PWM controller is represented by D. For the system shown in the Fig3.1, the equivalent load resistance of PEMFC can be expressed according to the knowledge of power electronic technology as.

$$R_{\mathrm{eq}} = \frac{U}{I} = (1 - D)^2 R_{\mathrm{L}} \tag{21}$$

In which Req is the equivalent load resistance of PEMFC, and RL denotes the actual load resistance, that is, the load resistance at the output of the Boost converter. It is well known that the output power of an electric source can reach its maximum if and only if its external resistance is equal to its internal resistance. According to eq (21), the equivalent load resistance can be adjusted by varying the duty cycle of the Boost converter. Therefore, by adjusting the duty cycle, the equivalent load resistance of the PEMFC can equal its internal resistance, thereby achieving maximum power output. [18]

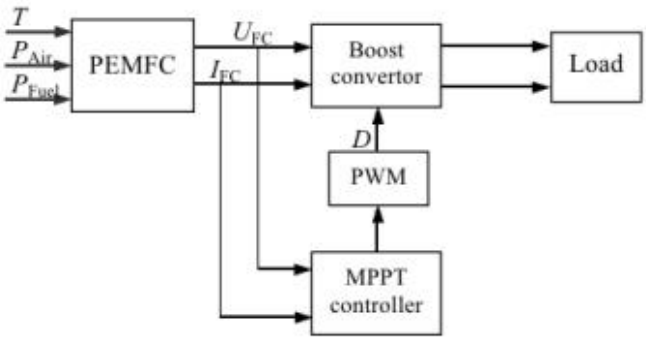

Fig 3.1: Diagram of the MPPT control system of PEMFC

A polarization curve can demonstrate a relationship between the cell voltage and the current density of a hydrogen cell in a steady state. Cell heat, partial pressures of hydrogen and oxygen, and membrane water content fuel cell characteristics, such as temperature (T), are variables that affect this curve. Both the voltage-current and power-current curves are impacted by hydrogen partial pressure (PH_2) and particulate oxygen pressure (PO_2), respectively. Fuel cell power and

voltage-current graphs are shown in Fig 3.2 Voltage drops caused by activation, concentration, and ohmic losses give FC its drooping properties. The FC output voltage is defined by such dips, as described by Larminie, Dicks, and McDonald in 2003. [19]

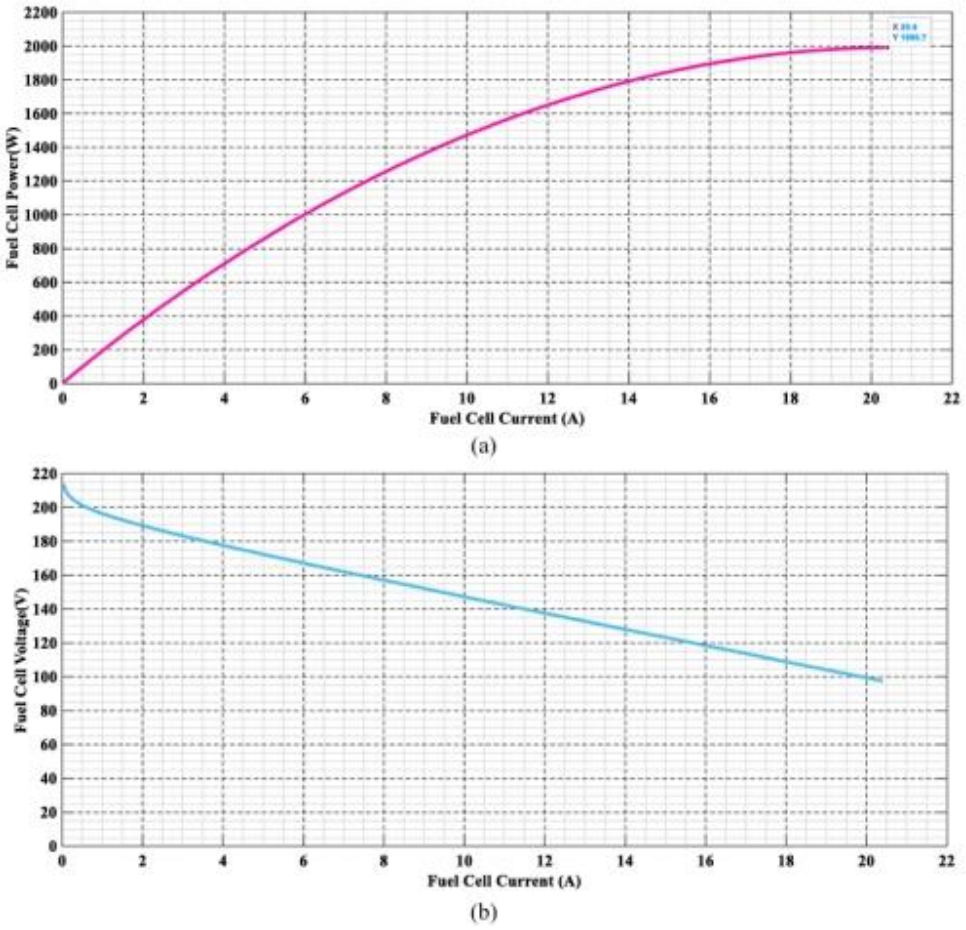

Fig 3.2: (a) The fuel cell's power-current and (b) its voltage-current trait.

3.2Development of Different PowerPoint Tracking Methods:

Due to the nonlinear characteristics of the fuel stack, the maximum power extraction from the source is very difficult. So, MPPT technology plays an important role in tracking the fuel stack of MPP position at different water membranes and operating temperature conditions. It was identified that the general power point tracing methodologies are not suitable for rapid changes in operating temperature conditions of the fuel stack. The conventional MPPT controllers' disadvantages are high output voltage fluctuations, more time for extracting the maximum output

voltage, high convergence time, plus needed a greater number of sensing devices. [20]

3.2.1P&O Algorithm.

P&O is the most widely used MPPT method at present. Its basic principle is to apply a positive disturbance voltage to the fuel cell, sample its output voltage and current, and calculate the change rate of its voltage and power. If the output power increases after the disturbance, it indicates that the direction of the disturbance voltage is the direction of the increase in the power output, and the disturbance should be continued in this direction; otherwise, the disturbance should be in the opposite direction. According to the changing direction of voltage and power, the disturbance voltage is continuously applied to the fuel cell until the maximum output power is approached gradually, to realize the MPPT. The flowchart of the P&O algorithm is shown in Fig3.3 in which “k” denotes the sampling point, and d stands for the increment of duty cycle. P&O has the advantages of simple calculation and convenient implementation, but it can only keep the system oscillating infinitely near the maximum power point, and can not accurately track the maximum power point, so it can not effectively solve the problems of tracking accuracy and speed.[18]

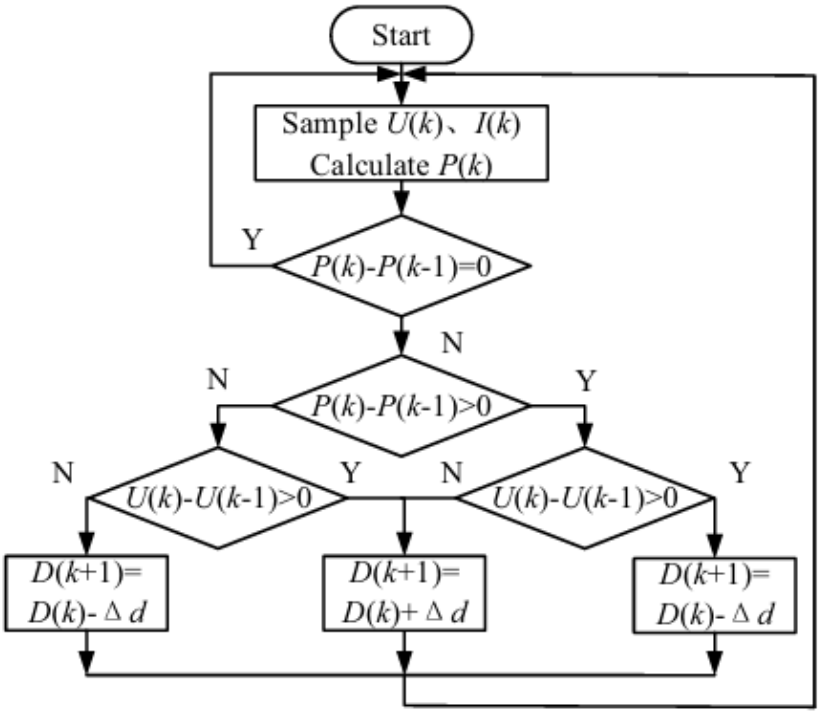

Fig 3.3**:** Flow chart of P&O algorithm of MFC.

3.2.2Artificial Intelligence:

Artificial Neural Networks (ANNs) are widely used in maximum power point tracking (MPPT) applications due to their capability to model nonlinear systems without requiring an accurate mathematical model. Among the different ANN structures, the Radial Basis Function Network (RBFN) is selected in this work because of its effectiveness in approximating nonlinear functions and its relatively fast convergence. The RBFN is based on radial basis functions in the hidden layer, which enables a localized and accurate mapping between the input and output variables. This characteristic makes it suitable for estimating the maximum power point of PEM fuel cell systems. Moreover, the network can be used to create a suitable duty cycle for the DC–DC converter, which helps with efficient power extraction, even when operating conditions change.[21]

3.2.2.1Functional Network-Based MPPT Controller:

Mostly, the ANN is used in nonlinear decision-making problems applications. These networks are implemented from the inspiration of biological neurons, and the ANN is designed from the combination of activation functions, mathematical operations, and optimization methodologies. In the article, the RBFN model neural controller is interfaced in the automotive fuel stack system to improve the dynamic behavior of EVs66. The RBF networks have the capability of approximation of complex functions, good modeling of nonlinear relationships, plus capturing the complex patterns from the available data to determine the accurate MPP position of the fuel stack. The RBF-related power point identifying the network working nature is illustrated in Fig1.10 Based on Fig1.10, the radial function is used as an activation function for obtaining the desirable duty to the DC–DC converter circuit. The RBF demonstrates the smooth transition from the center point to the surroundings of the neurons to adapt to the source space very efficiently. Based on available data sets, the RBF interpolates the input-output relations, and it generalizes the input-output relations for non-available data. The major advantage of RBF is its high computational efficiency. [22]

$$\mathrm{net}_{\mathrm{T}}^{(1)} = \mathrm{S}_{\mathrm{T}}^{1}(\mathrm{x}); \mathrm{x} = 1,2,3,4, \dots, \mathrm{n} \tag{22}$$

$$\mathrm{H}_{\mathrm{L}}^{(1)}(\mathrm{x}) = \mathrm{f}_{\mathrm{T}}^{(1)}\left(\mathrm{net}_{\mathrm{T}}^{(1)}(\mathrm{x})\right) = \mathrm{net}_{\mathrm{T}}^{1}(\mathrm{x}); \mathrm{T} = 1,2,3 \tag{23}$$

$$\mathrm{H}_{\mathrm{L}}^{(1)}(\mathrm{x}) = \mathrm{f}_{\mathrm{T}}^{(1)}\left(\mathrm{net}_{\mathrm{T}}^{(1)}(\mathrm{x})\right) = \mathrm{net}_{\mathrm{T}}^{1}(\mathrm{x}); \mathrm{T} = 1,2,3 \tag{24}$$

$$\mathrm{H}_{\mathrm{Y}}^{(2)}(\mathrm{x}) = \mathrm{f}_{\mathrm{Y}}^{(2)}\left(\mathrm{net}_{\mathrm{Y}}^{(2)}(\mathrm{x})\right); \mathrm{Y} = 1,2,3,4, \dots, 9 \tag{25}$$

$$\mu_{\mathrm{Y}} = [\mu_{1\mathrm{Y}} \quad \mu_{2\mathrm{Y}} \quad \mu_{3\mathrm{Y}} \quad \dots \quad \dots \quad \mu_{\mathrm{TY}}] \tag{26}$$

$$\sum_{\mathrm{Y}} = \mathrm{diag}[\ {}^{1}/?_{1\mathrm{Y}}^{2} \quad {}^{1}/?_{2\mathrm{Y}}^{2} \quad {}^{1}/?_{3\mathrm{Y}}^{2} \dots \dots . \quad {}^{1}/\sigma_{\mathrm{LM}}^{2}] \tag{27}$$

$$\mathrm{net}_{\mathrm{U}}^{(3)} = \sum_{\mathrm{U}} \mathrm{W}_{\mathrm{Y}}\mathrm{H}_{\mathrm{Y}}^{2}(\mathrm{x}); \mathrm{x} = 1,2,3,4,5, \dots \dots, \mathrm{n} \tag{28}$$

$$O_U^{(3)}(x) = f_U^{(3)}\left((net_U^3(x)) = net_U^3(x)\right) \quad (29)$$

Where the terms **T**, **U**, and Y are the first layer, output layer, plus the middle layers. The variables $\mathbf{S_T^1(x)}$, net $_{\mathbf{T}}^{(\mathbf{1})}(\mathbf{x})$ represents the net value of the source layer, and its corresponding output signal. The total selected data samples are identified as ' $\boldsymbol{x}$ '. The $\boldsymbol{H_L^{(1)}(x), H_Y^{(2)}(x)}$ gives the center layer the first and second node overall input signal. The hidden layer output net value is determined as net $_{\mathbf{Y}}^{(\mathbf{2})}(\mathbf{x})$. The variables ' S ', μ, ?, W, and O are indicated as input vectors, the mean value of the signal, controller coefficient, neuron weight, and required RBF output signal. [20]

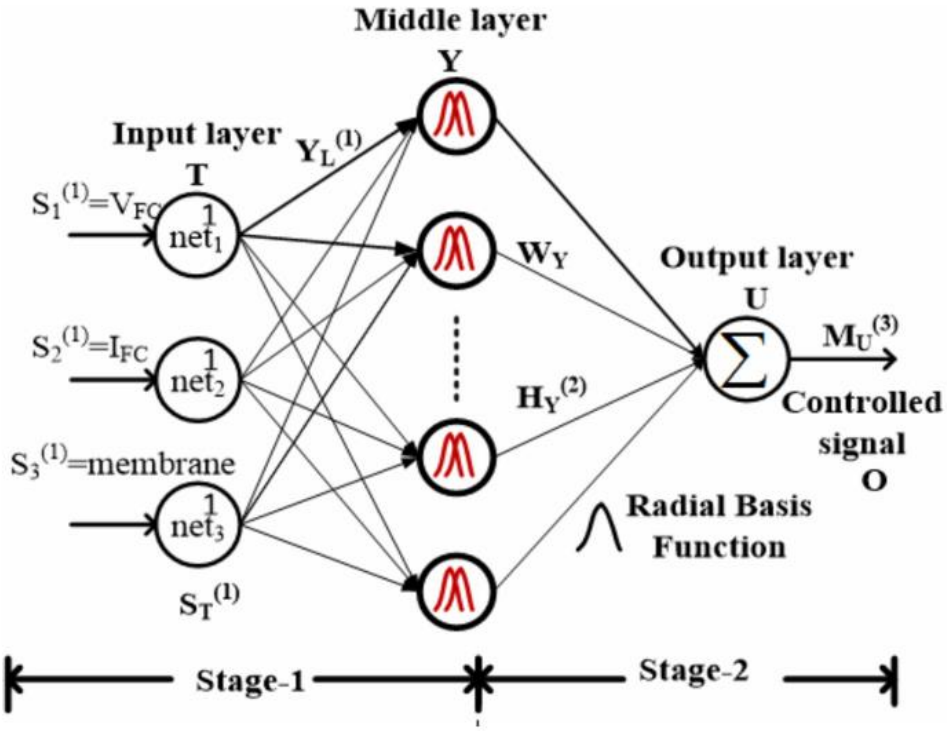

Fig 3.4**:** RBFN work process for PEMFC-based power supply system.

3.2.2.2Fuzzy Logic Control:

Recently, fuzzy logic control has been used in the design of MPPT control systems, particularly in scenarios requiring resilience and simpler design. Modern control strategies, such as the proposed Fuzzy-Predictive Current Control (FC-PCC), are essential for optimizing power flow and improving converter efficiency in renewable energy systems, aligning with the advancements discussed by Zhang et al. In this case, exact knowledge of the specific model is not required. Nevertheless, it is critical for the designer to have an in-depth understanding of the PEMFC's behavior**.** Fig 1.11 displays a fuzzy controller block diagram. Processing the incoming signals and giving them a fuzzy value falls to the fuzzification block. Based on the understanding of the process, the set of guidelines lets one regulate a linguistic description of each variable. Making an interpretation of the data, considering the rules and their membership functions, falls on the inference process. The fuzzy information generated by the inference mechanism is transformed into non-fuzzy information using the defuzzification block that is beneficial for the control of the process., while it has two inputs, namely the error E(k) and the change in the error DE(k), and one output is the current step size ΔIref The DE mentioned in Eq (32) represents the change in error and is calculated using Eq (31), While E(K-1) represents the error at sampling time (K-1), Ifc, and Pfc represent the PEMFC output current and power respectively.

$$P_{FC}(k) = I_{FC}(k)V_{FC}(k) \tag{30}$$

$$E(k) = \frac{P_{FC}(k) - P_{FC}(k-1)}{I_{FC}(k) - I_{FC}(k-1)} \tag{31}$$

$$DE(k) = E(k) - E(k-1) \tag{32}$$

The fuzzy MPPT system consists of 25 rules, which are listed in Table 1.12. The output ΔIref is determined utilizing these rules, and the Mamdani interface with a maximum operation fuzzy combination rule after the input variables are translated into linguistic variables during the fuzzification process. Fuzzy logic membership is shown in Fig 1.13 During the defuzzification process, the center of gravity approach is used to extract a numerical value from the output variable, as defined by the following eq. [23]

$$\Delta I_{ref} = \frac{\sum_{j=1}^{n} u\left(\Delta I_{ref_j}\right) - \Delta I_{ref_j}}{\sum_{j=1}^{n} u\left(\Delta I_{ref_j}\right)} \quad (33)$$

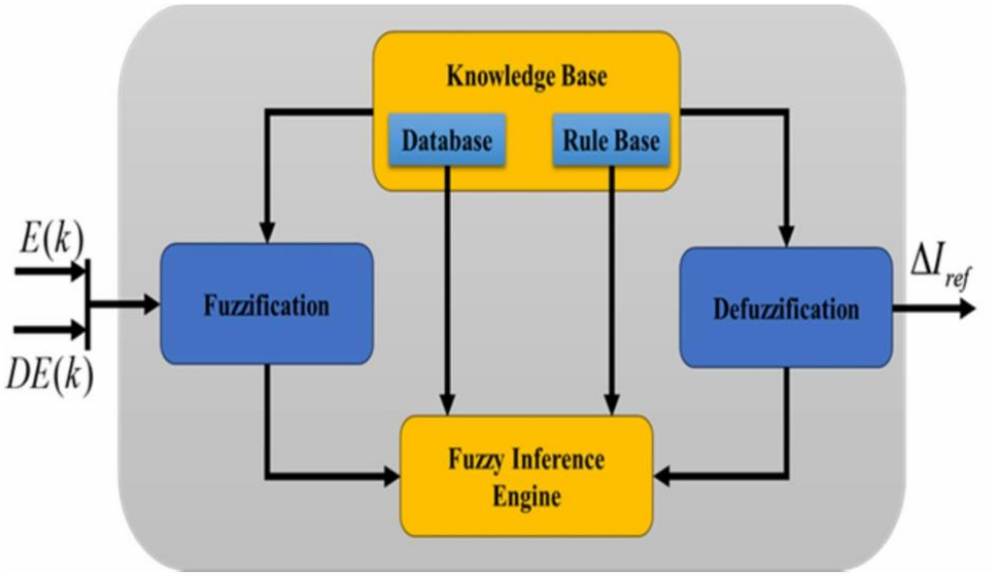

Fig3.5**:** Fuzzy current control diagram

E					
	nb	**ns**	**z**	**ps**	**pb**
DE					
nb	pb	ps	z	z	z
ns	pb	ps	z	z	ns
z	pb	ps	z	ns	nb
ps	ps	z	z	ns	nb
pb	z	z	z	ns	nb

Table 3.6: Fuzzy logic rules.

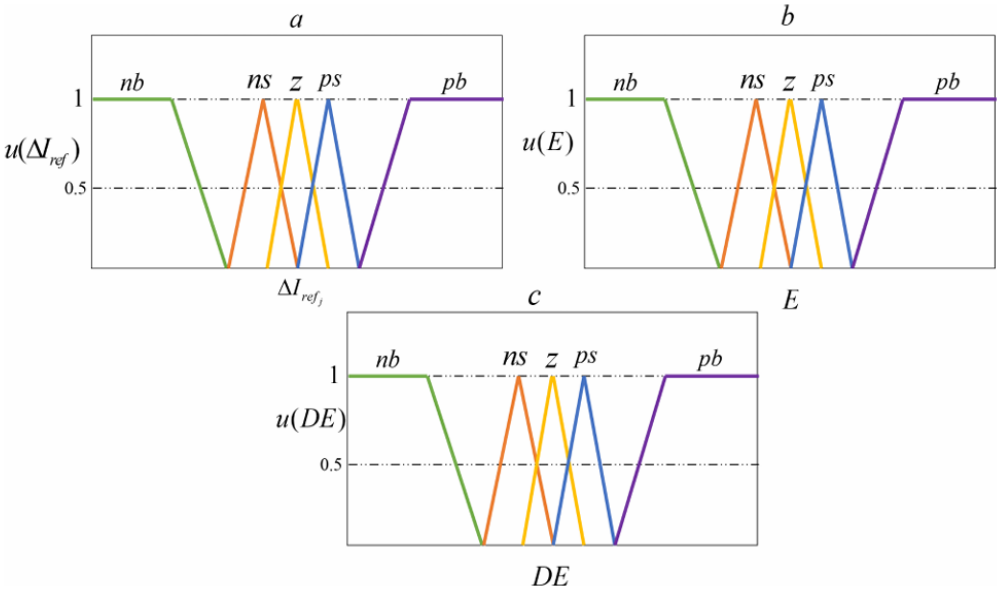

Fig 3.7: Fuzzy logic membership (a) output ΔIref, (b) input E, and (c) input DE.

3.3 Hybrid ANN–P&O Based Maximum Power Point Tracking for PEM Fuel Cell Systems :

Artificial Neural Network (ANN) and Perturb and Observe (P&O) algorithms in combination provide an effective hybrid approach for maximum power point tracking (MPPT) in PEM fuel cell (PEMFC) systems. In this method, the ANN is used for fast estimation of the optimal operating point for the measured variables like voltage, current, temperature, and gas pressure. Then, the P&O algorithm refines around the estimated point to extract maximum available power from the fuel cell. Especially, the ANN is well suited to handle the strong nonlinearity behavior and complex dynamics of PEMFC systems. Conversely, the P&O algorithm is simple, easy to implement, and effective for local optimization with a reduced steady-state error.[24]

The hybrid approach offers an improved dynamic response compared to the use of P&O alone, specifically in the case of load variations or changing operating conditions.

It also reduces the oscillations around the maximum power point thus improving the stabilityandefficiencyofthesystem. In sudden disturbances the ANN gives a fast and

reliable preliminary reference value which is progressively improved by P&O. Therefore, the combination of the two techniques provides a trade-off between fast convergence and high tracking accuracy. Therefore, the hybrid ANN – P&O MPPT method is regarded as a feasible and effective method to enhance the performance of PEMFC based power systems.[25]

Conclusion:

Maximum Power Point Tracking (MPPT) techniques play a fundamental role in improving the efficiency and performance of fuel cell energy systems by ensuring operation at the optimal power point under varying conditions. Different MPPT approaches were analyzed, including conventional and intelligent methods. The Perturb and Observe (P&O) algorithm was presented as a simple and widely used technique due to its ease of implementation and satisfactory tracking capability. However, its performance may be affected by steady-state oscillations and slow response under rapid operating variations.[26]

Artificial intelligence-based methods were also investigated, particularly Artificial Neural Networks (ANN) and Fuzzy Logic controllers. These intelligent approaches provide enhanced adaptability and better dynamic performance compared to classical methods. ANN techniques are capable of learning nonlinear system behavior and improving tracking accuracy, while Fuzzy Logic offers robust decision-making without requiring an accurate mathematical model. The comparative study highlights the importance of advanced MPPT strategies for achieving higher efficiency, improved stability, and optimized energy extraction in PEMFC systems.[27]

ChapterVI:Simultion and Performance Analysis of Hybrid MPPT Techniques For PEMFC Systems

ChapterⅥ:Simultion and Performance Analysis of Hybrid MPPT Techniques For PEMFC Systems:

Introduction:

In this chapter a hybrid Maximum Power Point Tracking (MPPT) controller for Proton Exchange Membrane Fuel Cell (PEMFC) system is developed and simulated. The proposed method combines the conventional Perturb and Observe (P&O) algorithm with an Artificial Neural Network (ANN) to take advantage of the advantages of both techniques .[28]

The main goal of this hybrid approach is to achieve more accurate maximum power point tracking, reduce power pulsations and improve the dynamic performance of the fuel cell under different operating conditions. The complete system including PEMFC model, DC-DC boost converter and control algorithm is implemented and tested in MATLAB/Simulink to evaluate the system behavior and verify the effectiveness of the proposed controller.[29]

4.1. PEMFC Simulation Model:

The training dataset was created to evaluate the efficiency of a Proton Exchange Membrane Fuel Cell (PEMFC) stack. The stack design, operating circumstances, control settings, and performance measures were selected for accurate assessment and validation. These variables comprised the quantity and layouto ff fuel cells, temperature ,pressure, andhumidity.midity, fuel flow rate, air supply, cooling, and voltage control. The technique's efficiency was tested using relevant measures, including power output, current density, and voltage efficiency. Using these settings, the suggested approach was assessed and verified to maximize the performance of the PEMFC stack under certain operating circumstances and control parameters. In Fig 4.2,Fig 4.3, various parameters and corresponding values for a fuel cell system are presented. The table provides important information about the system’s characteristics and operational conditions.[30]

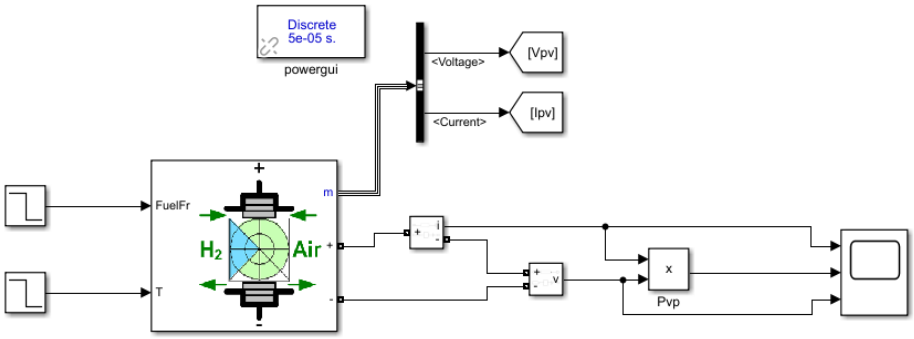

Fig 4.1 : Simulink Model Of The PEMFC System

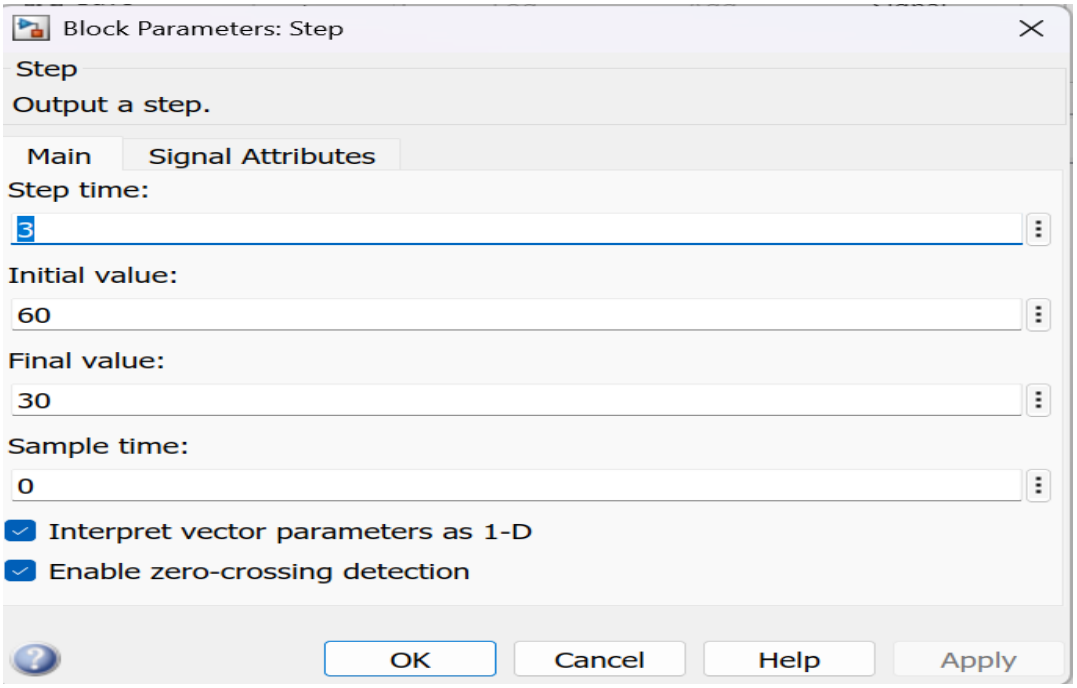

Fig 4.2: Step Block Parameters Configuration In Simulink.

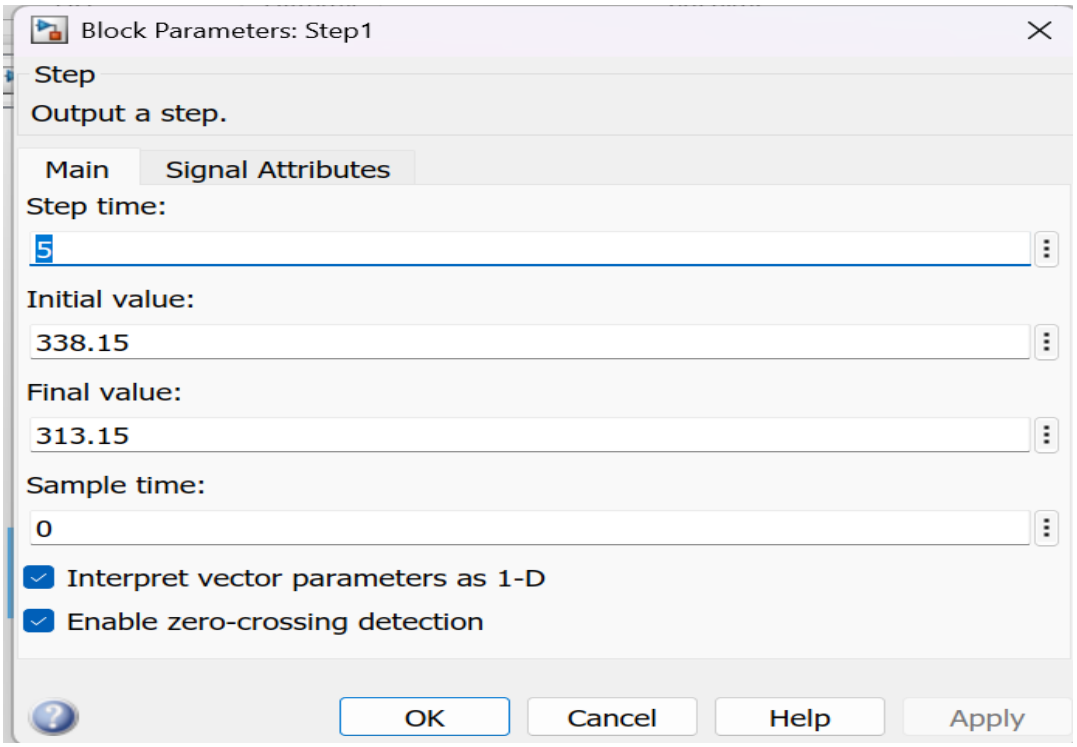

Fig 4.3: Step1 Block Parameters Configuration in Simulink.

4.2. Modeling of the Boost DC-DC Converter :

The PEMFC output voltage was increased and regulated by the DC-DC boost converter. The converter consists of an inductor (L), a MOSFET switch, a diode (D) and an output capacitor (C). During the switching process, the inductor stores energy and the capacitor reduces the voltage ripples at the output side . The switching pulses for the MOSFET gate were generated using a PWM (Pulse Width Modulation) technique. The pulse width was controlled according to the duty cycle, whereas the switching frequency determines the number of switching operations per second. Figure 4 illustrates the implemented DC-DC boost converter model. [31]

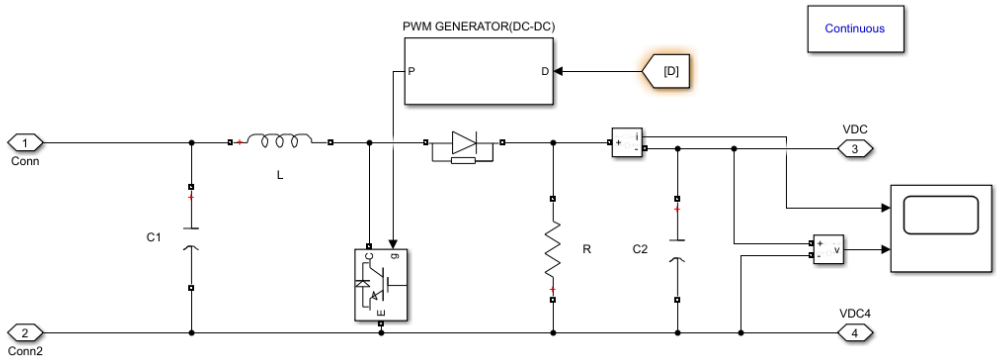

Fig4.4**:** Simulation of A DC-DC Boost Converter Using MATLAB/Simulink

Parameter	Value
Inductor L	1e-3 H
Input Capacitor C1	500e-6 µF
Output Capacitor C2	1e-3 µF
MOSFET Switching Frequency	5000 Hz
Load Resistance	10 Ohm

Table 4.5: DC-DC Boost Converter Parameters

:

V_0 is dependent on input voltage (Vi) and DU as stated in (34)

$$V_0 = \frac{1}{1-DU} * Vi \tag{34}$$

For known values of Vi and Vo, the value of DU can be derived from (35) as below:

$$DU = 1 - \frac{Vi}{Vo} \tag{35}$$

When the DC-DC boost converter is employed for MPPT of PEMFC, V_{sta} and V_{MP} represent Vi and Vo, respectively. Since Vsta and V_{MP} change continuously, then DU needs to be adjusted continuously. The suggested control strategy for adjusting the DU of the DC-DC boost converter for MPPT of PEM-FC is illustrated in the next section.[31]

A Pulse Width Modulation (PWM) technique was employed to generate switching pulses for the MOSFET gate of the DC-DC boost converter. The DU was continuously adjusted according to the MPPT control strategy to regulate the converter output voltage and ensure maximum power extraction from the PEMFC system.[34]

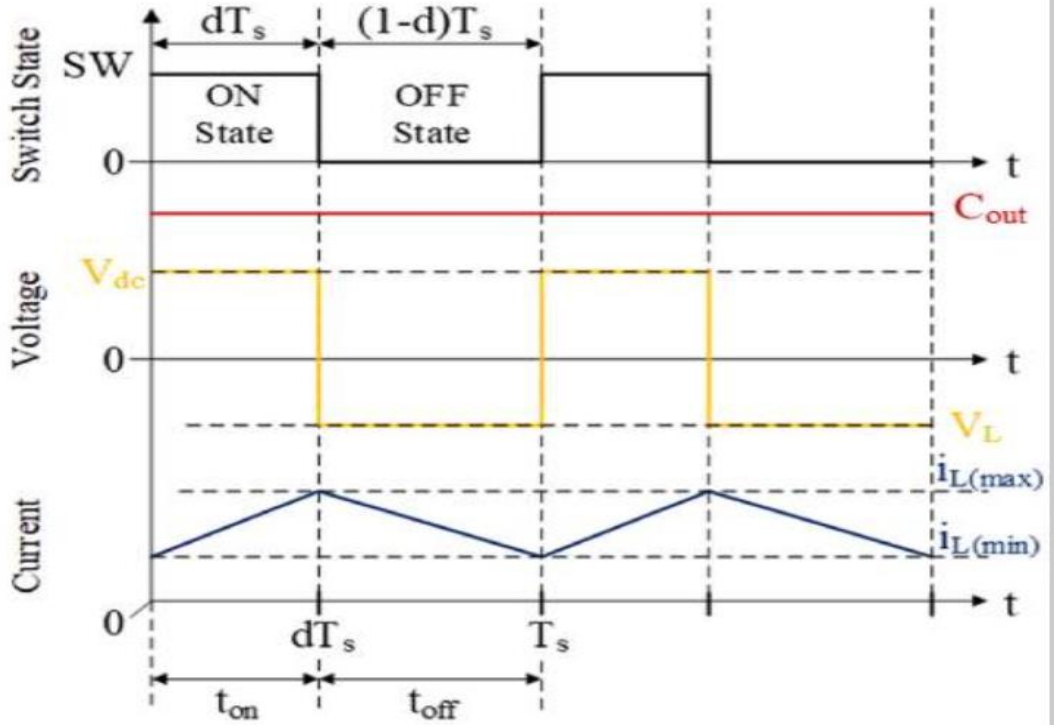

Fig 4.6: PWM Switching Waveform of The DC-DC Boost Converter.[23]

4.3 Hybrid MPPT Control Block :

4.3.1 Conventional P&O MPPT Algorithm:

The Perturb and Observe (P&O), amongst the MPPT techniques, is one of the most widely used because of its simple implementation and low computational complexity. The algorithm works by perturbing the duty cycle of the DC-DC boost converter and observing the change in the output power. If the power increases the perturbation is continued in the same direction otherwise the perturbation direction is reversed. In this way, the controller continuously tracks the maximum power point of the PEMFC system .[35]

The P&O MPPT algorithm was implemented in MATLAB/Simulink using a MATLAB Function block to generate the duty cycle of the DC-DC boost converter.

```
function D = MPPT_PO(V, I)
% Perturb and Observe (P&O) Maximum Power Point Tracking Algorithm
% Define persistent variables to hold values between simulation
steps
persistent V_prev P_prev D_prev
% Initialize variables during the first simulation step
if isempty(V_prev)
    V_prev = 0;
    P_prev = 0;
    D_prev = 0.5; % Start with a 50% duty cycle
end
% Step size (delta_D) - Optimized to 0.0005 to eliminate violent
oscillations
delta_D = 0.0005;
% Calculate current power
P = V * I;
% P&O Algorithm Logic
if (P - P_prev) ~= 0
    if (P - P_prev) > 0
        if (V - V_prev) > 0
            D = D_prev - delta_D;
        else
            D = D_prev + delta_D;
        end
    else
        if (V - V_prev) > 0
            D = D_prev + delta_D;
        else
            D = D_prev - delta_D;
        end
    end
else
    D = D_prev;
end
% Converter Protection: Saturation limits to prevent fuel cell
collapse
if D > 0.85
    D = 0.85; % Max limit lowered to protect the Fuel Cell
elseif D < 0.1
    D = 0.1;
end
% Update previous values for the next iteration
V_prev = V;
P_prev = P;
D_prev = D;
end
```

+

The P&O MPPT methodology implemented in MATLAB/ Simulink includes the following steps:

- Measurement of the PEMFC output voltage and current.
- Calculation of the output power.

- Comparison of the present and previous operating points.
- Adjustment of the perturbation direction according to the power variation.
- Generation of the duty cycle signal for the DC-DC boost converter using a PWM controller.
- Continuous tracking of the maximum power point of the PEMFC system.

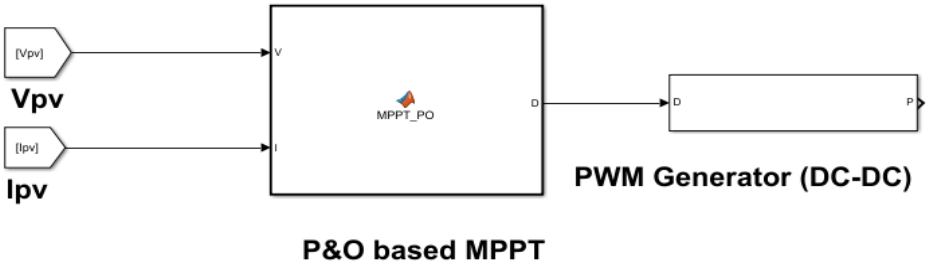

Fig 4.7 : Simulink Implementation of The Conventional P&O MPPT Controller.

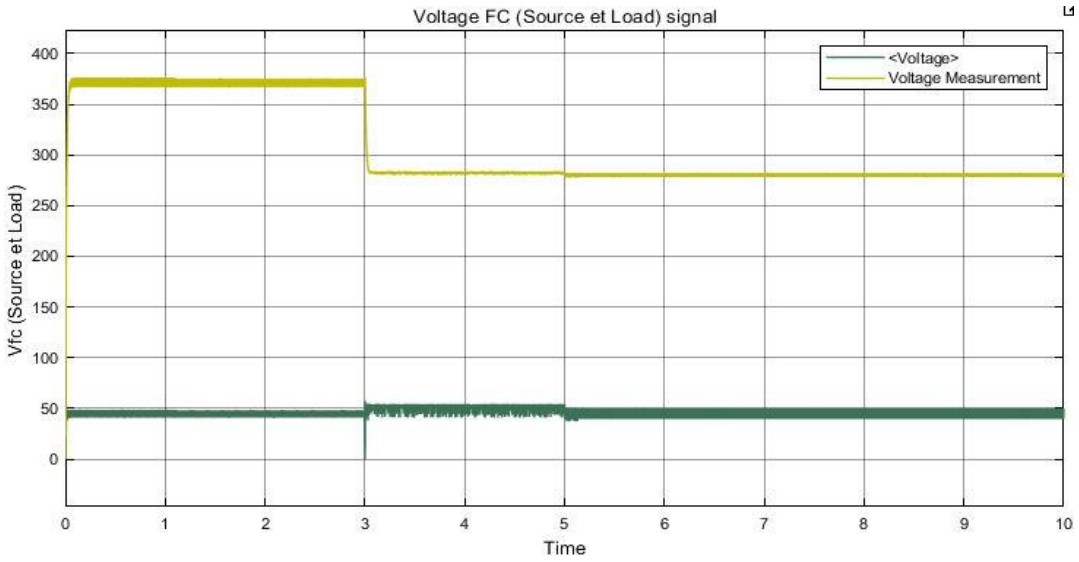

Fig 4.8:Voltage FC(Source Et Load) Signal

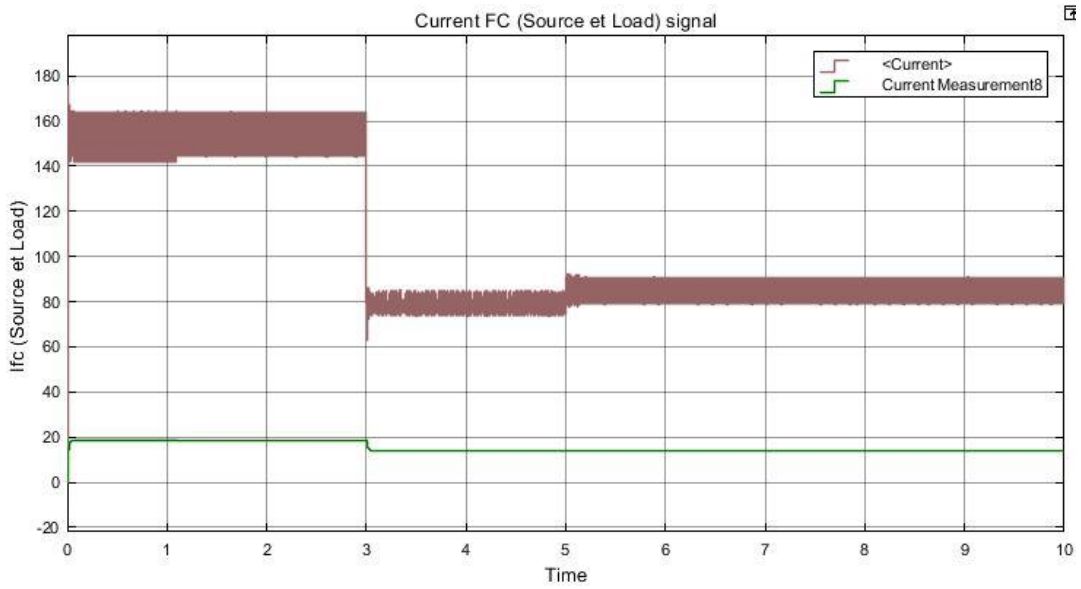

Fig 4.9: Current FC (Source Et Load) Signal

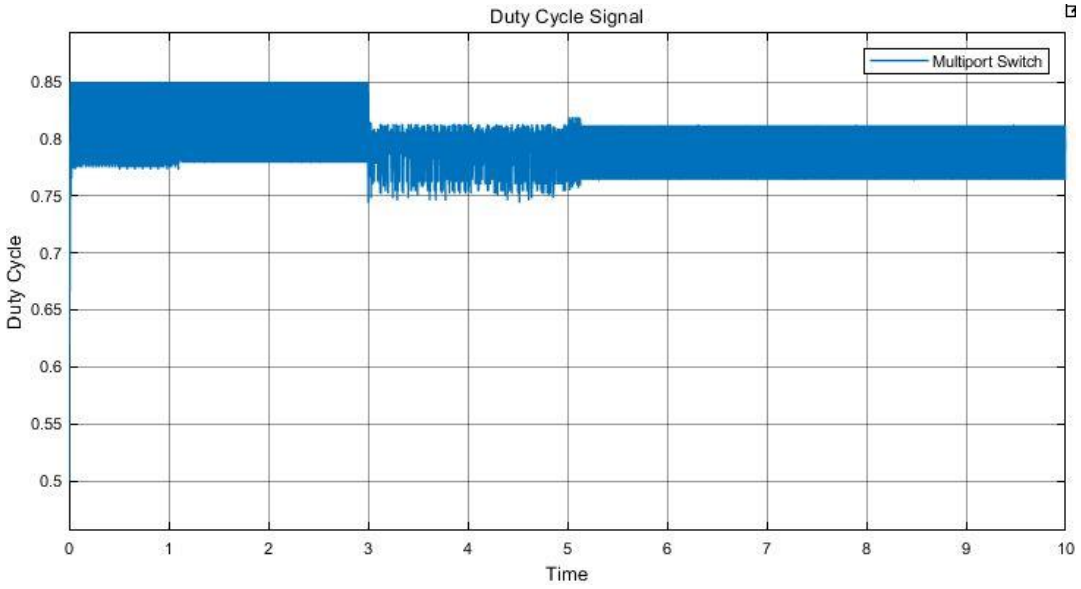

Fig 4.10: Duty Cycle Signal

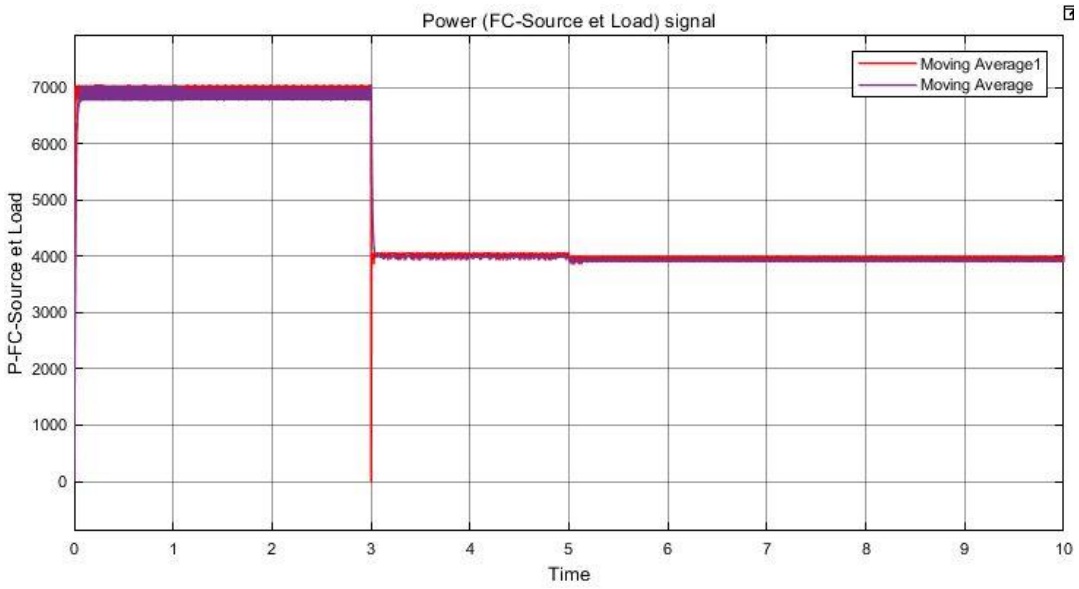

Fig 4.11:Power (Fc-Source Et Load) Signal

Fig4.8: Voltage FC (Source and Load) Signal

Scientific Analysis:

This figure illustrates the voltage response of the fuel cell stack (Vfc) and the load voltage under the conventional Perturb and Observe (P&O) MPPT controller.

The system started with a high load voltage of approximately 370 V, indicating stable initial operation. At (t = 3) seconds, a step load change was applied, causing the load voltage to drop to around 270 V. The controller responded relatively quickly, and the voltage stabilized within a short settling time.

Key Observations:

The response is acceptably fast; however, a slight ripple is noticeable after the transient period.

This ripple is a typical characteristic of the P&O method due to its continuous perturbation around the maximum power point.

The reference voltage (green curve) remains stable at approximately 45 V, demonstrating effective regulation of the fuel cell stack voltage.

Fig4.9: Current FC (Source and Load) Signal

Scientific Analysis:

This figure presents the fuel cell stack current (Ifc) and the load current.

In the initial phase (0–3 s), the system drew a high current from the fuel cell, ranging between 145–165 A. Following the load change at \(t = 3 \) s, the fuel cell

current decreased to approximately 85–95 A, accompanied by pronounced oscillations during the transient period (3–5 s). The load current remained stable at around 20 A.

Physical Interpretation:

The significant difference between source and load currents is expected in a Boost DC-DC converter, following the relationship .

The sustained oscillations in fuel cell current represent one of the major drawbacks of the conventional P&O algorithm. Such oscillations can increase stress on the fuel cell membrane and potentially reduce its lifespan.

Fig4.10: Duty Cycle Signal

Scientific Analysis:

This figure depicts the behavior of the duty cycle (D) of the DC-DC converter switch.

The duty cycle started at approximately 0.84, then decreased at (t = 3) s to a range of 0.76–0.81, exhibiting significant oscillations during the transient phase before settling around 0.80.

Control Perspective:

The variation in duty cycle is the primary mechanism by which the P&O algorithm searches for the maximum power point.

The persistent ripple observed in the duty cycle is an inherent feature of the classical P&O method, resulting from continuous small perturbations even after reaching the vicinity of the MPP.

A steady-state duty cycle of 0.80 corresponds to an appropriate voltage conversion ratio for stepping up the fuel cell voltage to the required load voltage level.

Fig 4.11: Power (FC-Source and Load) Signal

Scientific Analysis:

This figure shows the power extracted from the fuel cell source and delivered to the load.

The power started at approximately 7000 W, then experienced a sharp drop at (t = 3) s to a new steady-state level of 3900–4000 W, with minor fluctuations.

Interpretation:

The power reduction is consistent with the imposed load change.

The P&O controller successfully tracked a stable operating point near the maximum power point after the disturbance. Nevertheless, the presence of small oscillations indicates limited tracking precision compared to advanced intelligent controllers.

4.3.2 ANN – Based MPPT Controller:

An ANN-based MPPT controller was developed to improve the tracking performance of the PEMFC system under different operating conditions. The proposed controller is designed to reduce steady-state oscillations and improve the dynamic response compared with the conventional P&O technique.[36]

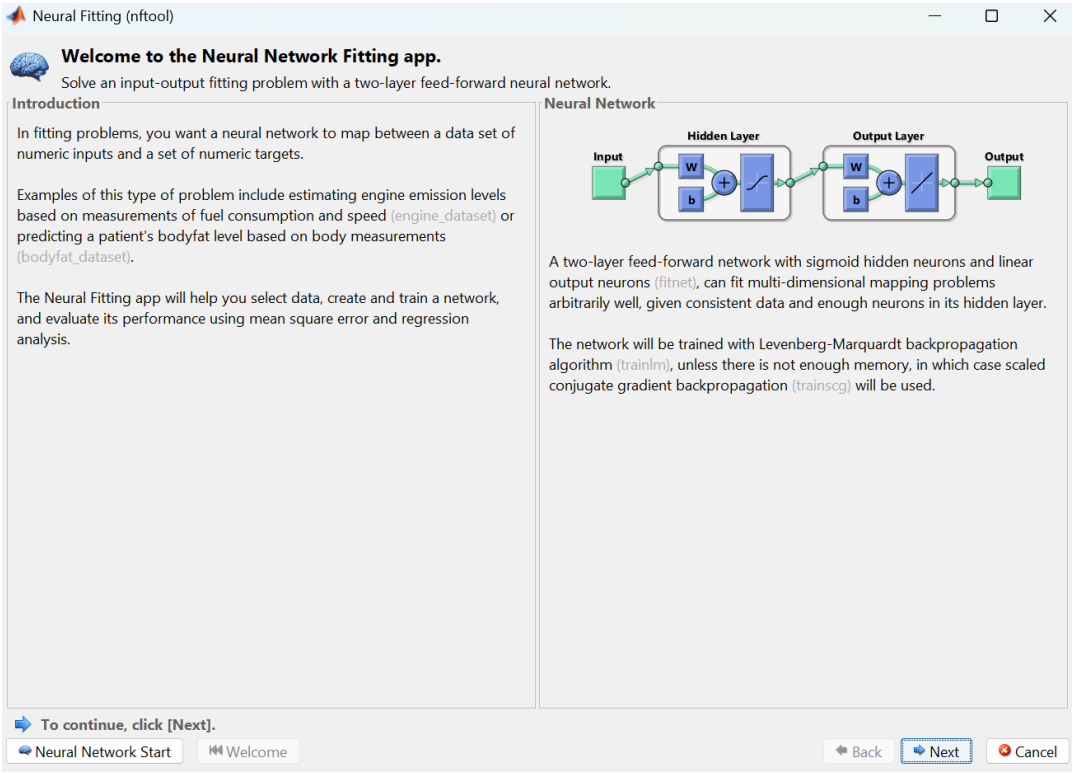

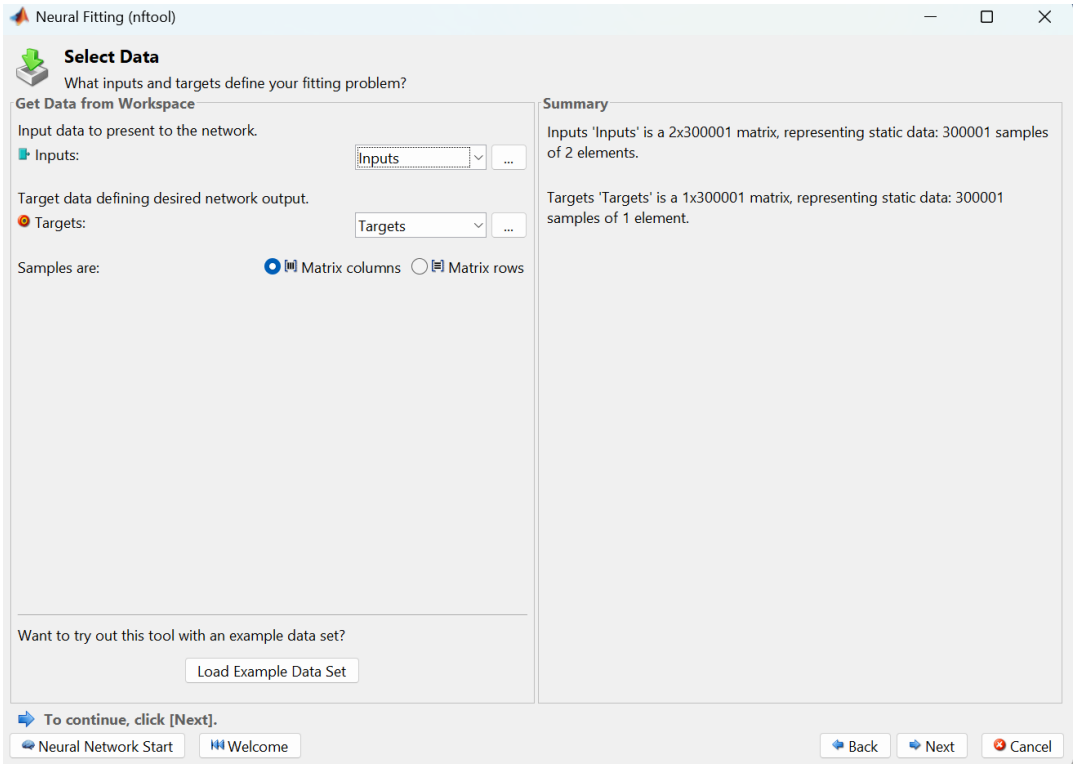
Neural Fitting (nftool)
Select Data
What inputs and targets define your fitting problem?
Get Data from Workspace
Input data to present to the network.
Inputs:
Inputs
Target data defining desired network output.
Targets:
Targets
Samples are:
Matrix columns
Matrix rows
Want to try out this tool with an example data set?
Load Example Data Set
Summary
Inputs 'Inputs' is a 2x300001 matrix, representing static data: 300001 samples of 2 elements.
Targets 'Targets' is a 1x300001 matrix, representing static data: 300001 samples of 1 element.
To continue, click [Next].
Neural Network Start
Welcome
Back
Next
Cancel

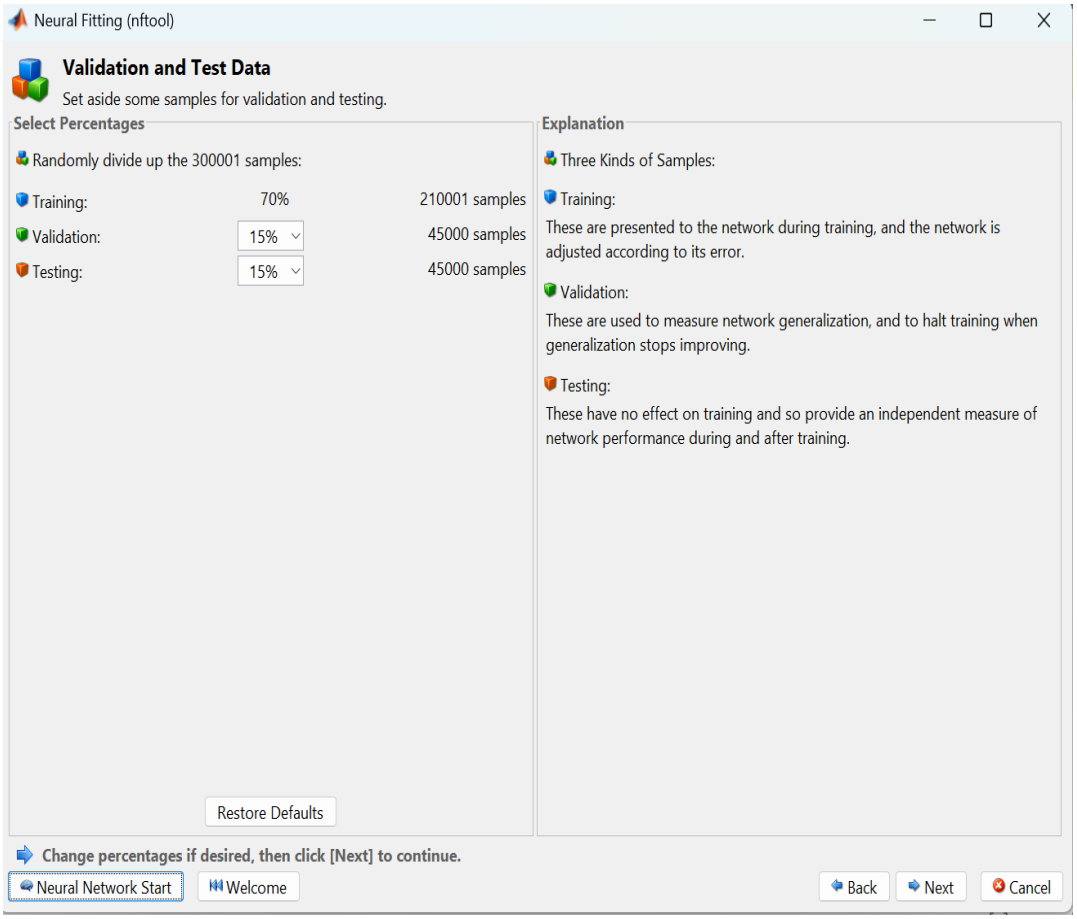
Neural Fitting (nftool)
Validation and Test Data
Set aside some samples for validation and testing.
Select Percentages
Randomly divide up the 300001 samples:
Training:
70%
210001 samples
Validation:
15%
45000 samples
Testing:
15%
45000 samples
Restore Defaults
Explanation
Three Kinds of Samples:
Training:
These are presented to the network during training, and the network is adjusted according to its error.
Validation:
These are used to measure network generalization, and to halt training when generalization stops improving.
Testing:
These have no effect on training and so provide an independent measure of network performance during and after training.
Change percentages if desired, then click [Next] to continue.
Neural Network Start
Welcome
Back
Next
Cancel

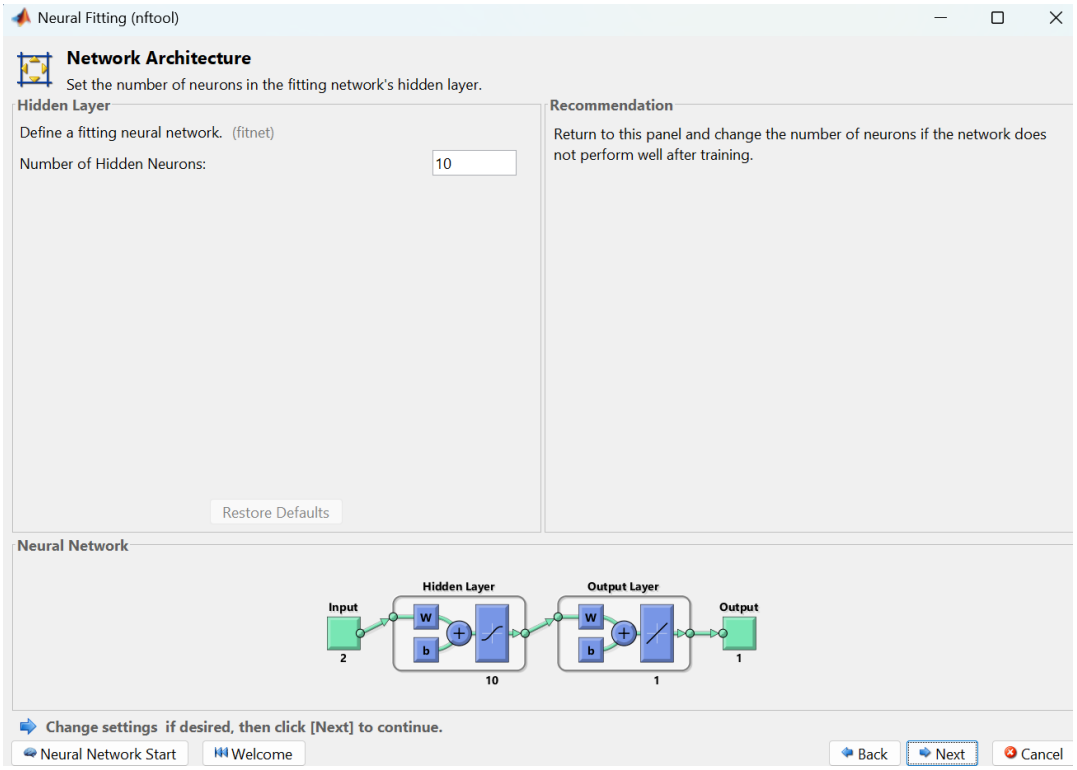
Neural Fitting (nftool)
Network Architecture
Set the number of neurons in the fitting network's hidden layer.
Hidden Layer
Define a fitting neural network. (fitnet)
Number of Hidden Neurons: 10
Restore Defaults
Recommendation
Return to this panel and change the number of neurons if the network does not perform well after training.
Neural Network
Input
2
Hidden Layer
W
b
10
Output Layer
W
b
1
Output
1
Change settings if desired, then click [Next] to continue.
Neural Network Start
Welcome
Back
Next
Cancel

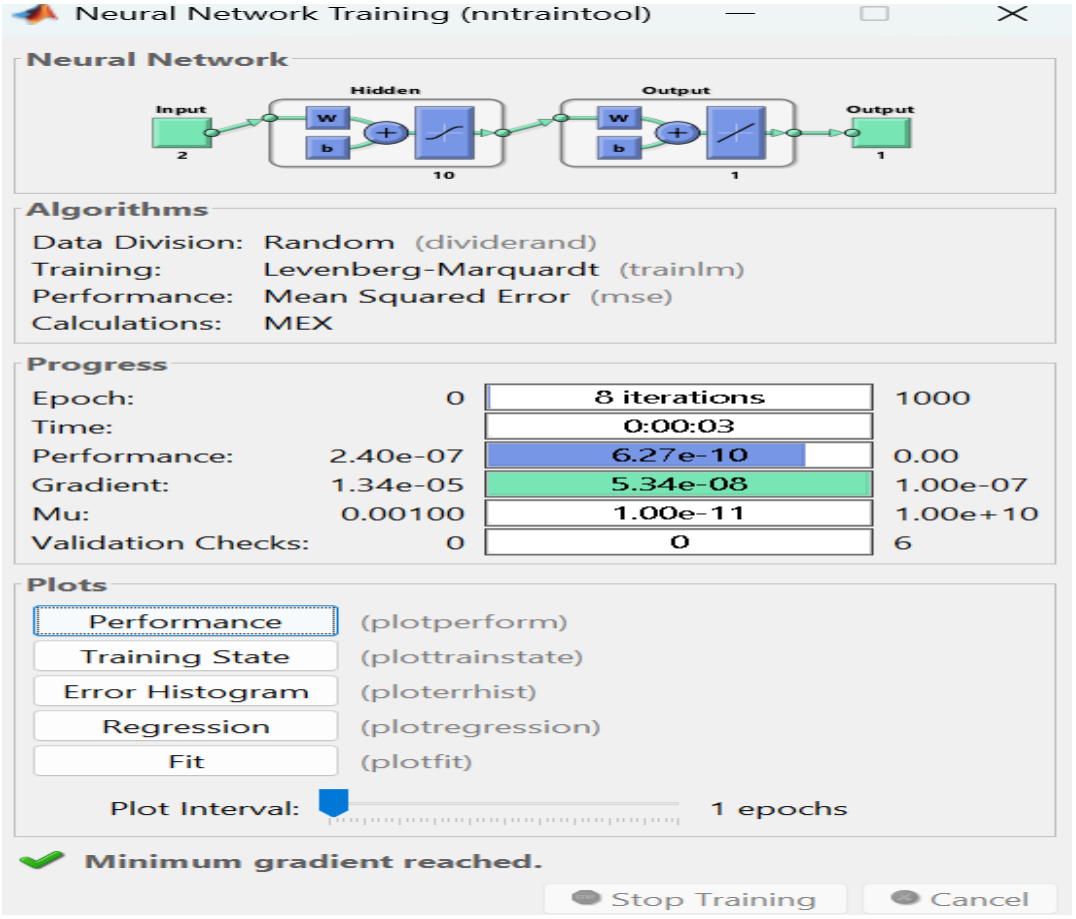
Neural Network Training (nntraintool)
Neural Network
Input
2
Hidden
W
b
10
Output
W
b
1
Output
1
Algorithms
Data Division: Random (dividerand)
Training: Levenberg-Marquardt (trainlm)
Performance: Mean Squared Error (mse)
Calculations: MEX
Progress
Epoch: 0 8 iterations 1000
Time: 0:00:03
Performance: 2.40e-07 6.27e-10 0.00
Gradient: 1.34e-05 5.34e-08 1.00e-07
Mu: 0.00100 1.00e-11 1.00e+10
Validation Checks: 0 0 6
Plots
Performance (plotperform)
Training State (plottrainstate)
Error Histogram (ploterrhist)
Regression (plotregression)
Fit (plotfit)
Plot Interval: 1 epochs
Minimum gradient reached.
Stop Training
Cancel

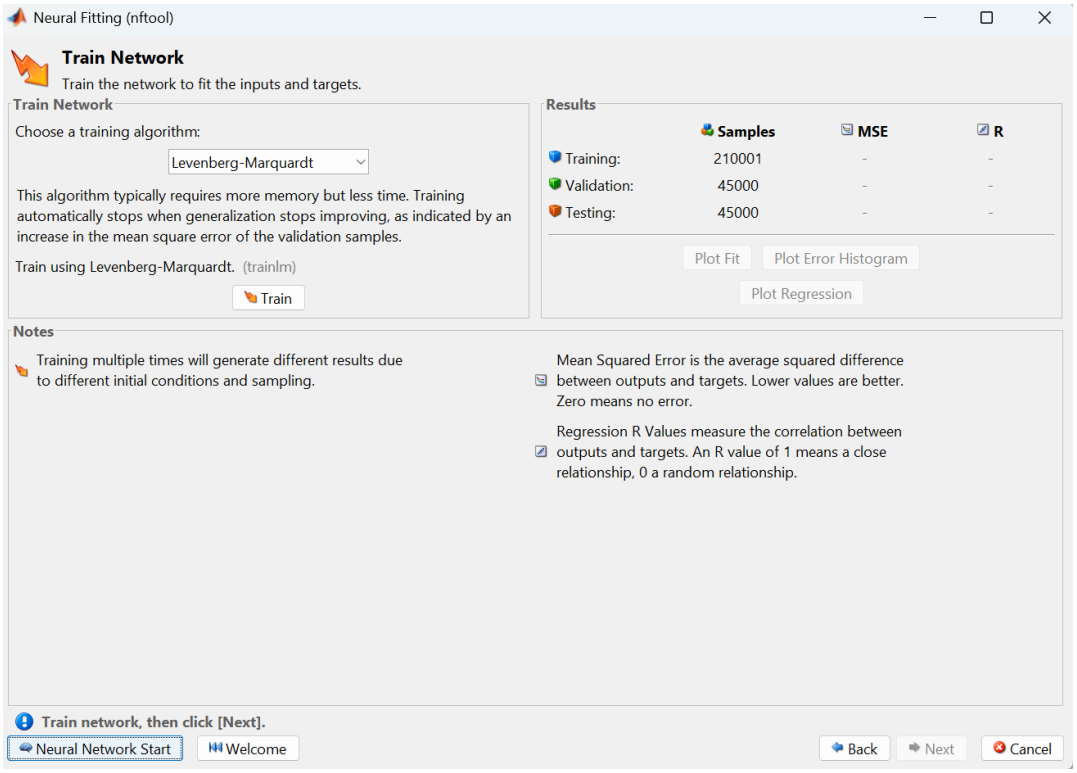
Neural Fitting (nftool)
Train Network
Train the network to fit the inputs and targets.
Train Network
Choose a training algorithm:
Levenberg-Marquardt
This algorithm typically requires more memory but less time. Training automatically stops when generalization stops improving, as indicated by an increase in the mean square error of the validation samples.
Train using Levenberg-Marquardt. (trainlm)
Train
Results
Samples
MSE
R
Training: 210001 - -
Validation: 45000 - -
Testing: 45000 - -
Plot Fit
Plot Error Histogram
Plot Regression
Notes
Training multiple times will generate different results due to different initial conditions and sampling.
Mean Squared Error is the average squared difference between outputs and targets. Lower values are better. Zero means no error.
Regression R Values measure the correlation between outputs and targets. An R value of 1 means a close relationship, 0 a random relationship.
Train network, then click [Next].
Neural Network Start
Welcome
Back
Next
Cancel

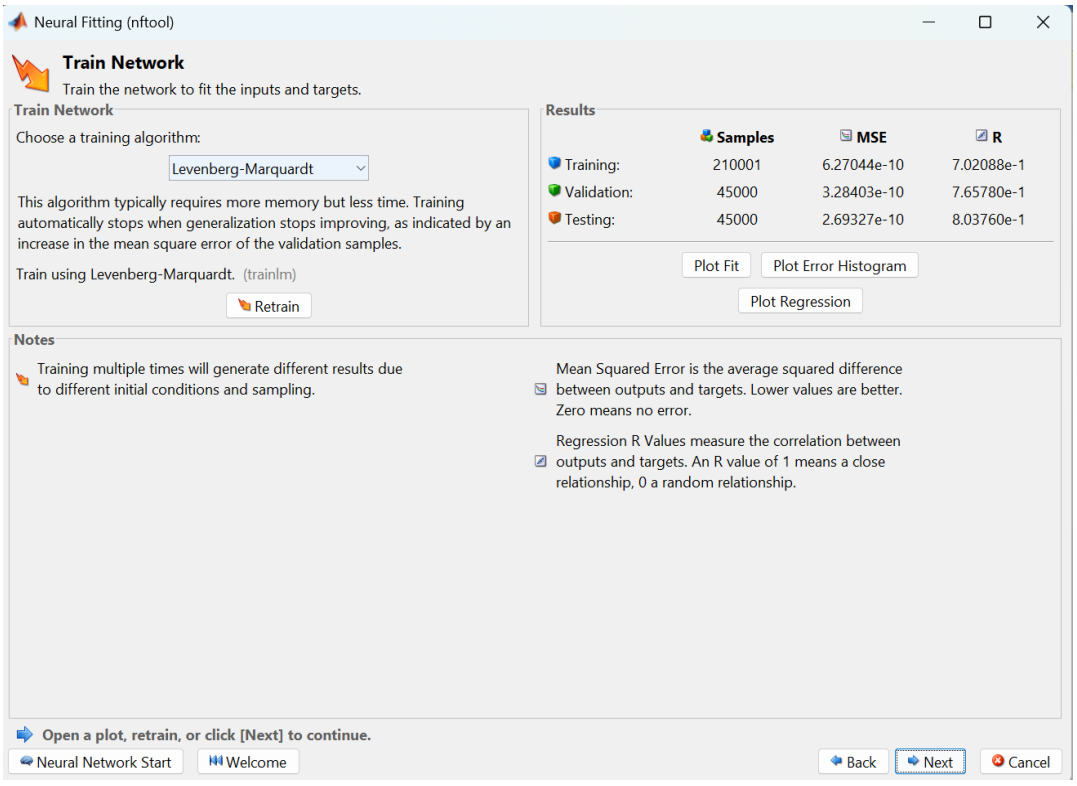
Neural Fitting (nftool)
Train Network
Train the network to fit the inputs and targets.
Train Network
Choose a training algorithm:
Levenberg-Marquardt
This algorithm typically requires more memory but less time. Training automatically stops when generalization stops improving, as indicated by an increase in the mean square error of the validation samples.
Train using Levenberg-Marquardt. (trainlm)
Retrain
Results
Samples
MSE
R
Training: 210001 6.27044e-10 7.02088e-1
Validation: 45000 3.28403e-10 7.65780e-1
Testing: 45000 2.69327e-10 8.03760e-1
Plot Fit
Plot Error Histogram
Plot Regression
Notes
Training multiple times will generate different results due to different initial conditions and sampling.
Mean Squared Error is the average squared difference between outputs and targets. Lower values are better. Zero means no error.
Regression R Values measure the correlation between outputs and targets. An R value of 1 means a close relationship, 0 a random relationship.
Open a plot, retrain, or click [Next] to continue.
Neural Network Start
Welcome
Back
Next
Cancel

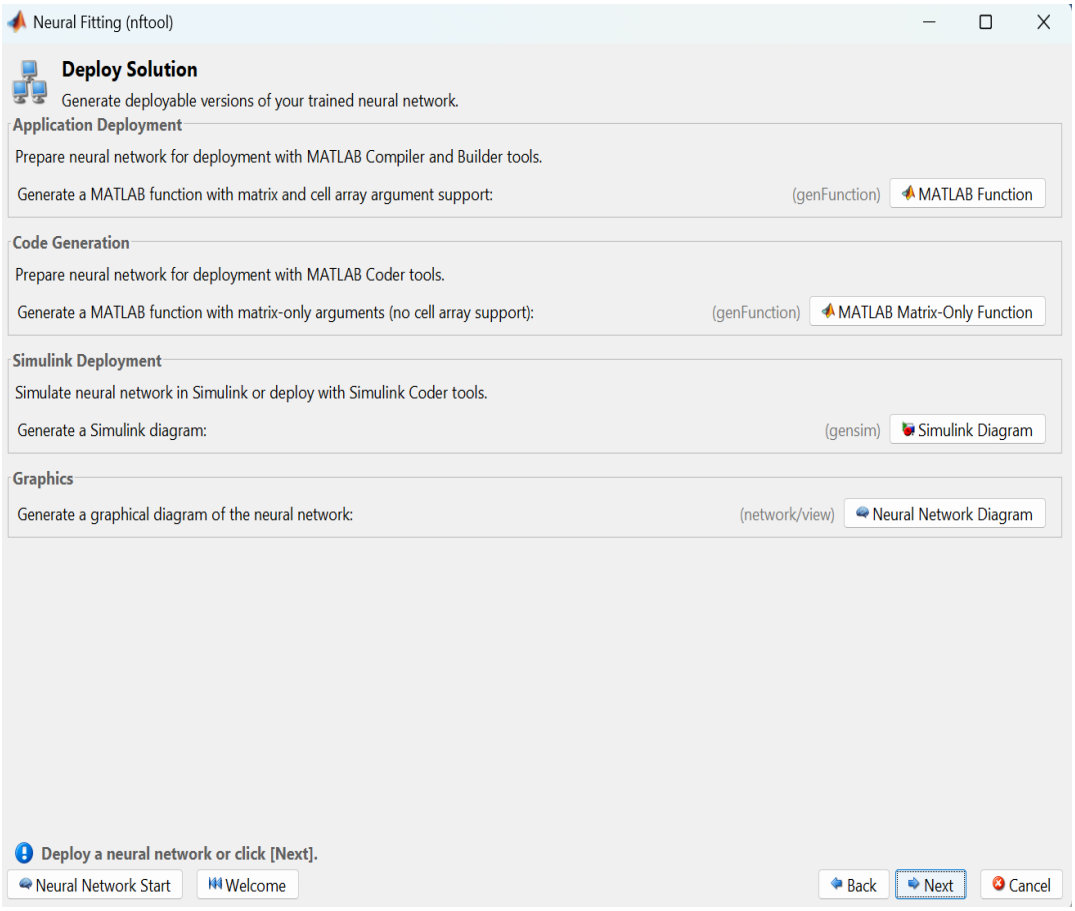

The ANN training methodology adopted for the proposed MPPT controller includes the following stages:

- Generation of the training dataset using the PEMFC simulation model under different operating conditions.
- Extraction of the PEMFC voltage, current, and duty cycle data from MATLAB/Simulink.
- Preparation of the input and target datasets using the following MATLAB commands:
- MATLAB

```
Inputs = [Vfc.Data, Ifc.Data]';

Targets = D.Data';
```

- Implementation of the Neural Network Fitting Tool (nftool) for ANN configuration and training.
- Automatic division of the dataset into training, validation, and testing subsets using the default MATLAB ratios of 70%, 15%, and 15%, respectively.
- Adoption of a feedforward neural network architecture with 10 hidden neurons to improve MPPT tracking accuracy.
- Training of the ANN model using the Levenberg–Marquardt backpropagation algorithm to minimize the Mean Squared Error (MSE).
- Evaluation of the ANN model performance using regression analysis and training performance indicators.
- Integration of the trained ANN model into the PEMFC MPPT control system for optimal duty cycle prediction and continuous maximum power point tracking.

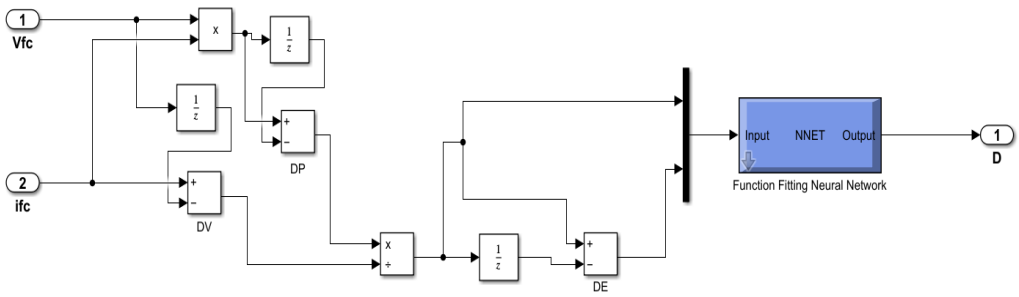

Fig 4.12: Simulink of The Implementation of The MPPT ANN

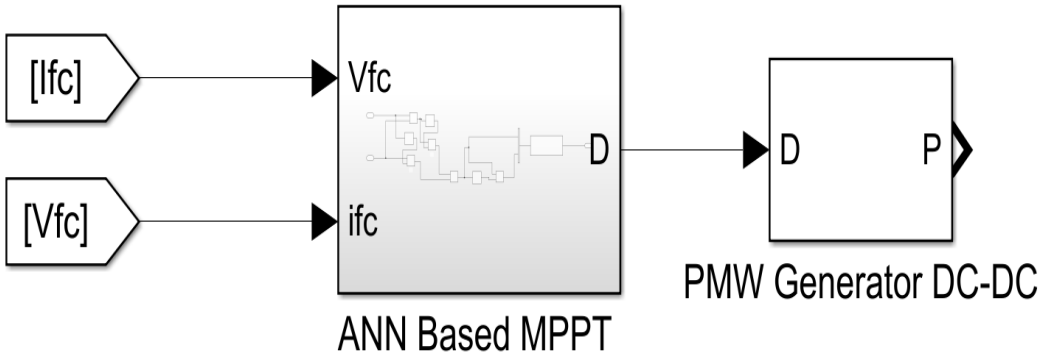

Fig 4.13: Simulink Implementation of The Conventional ANN MPPT Controller.

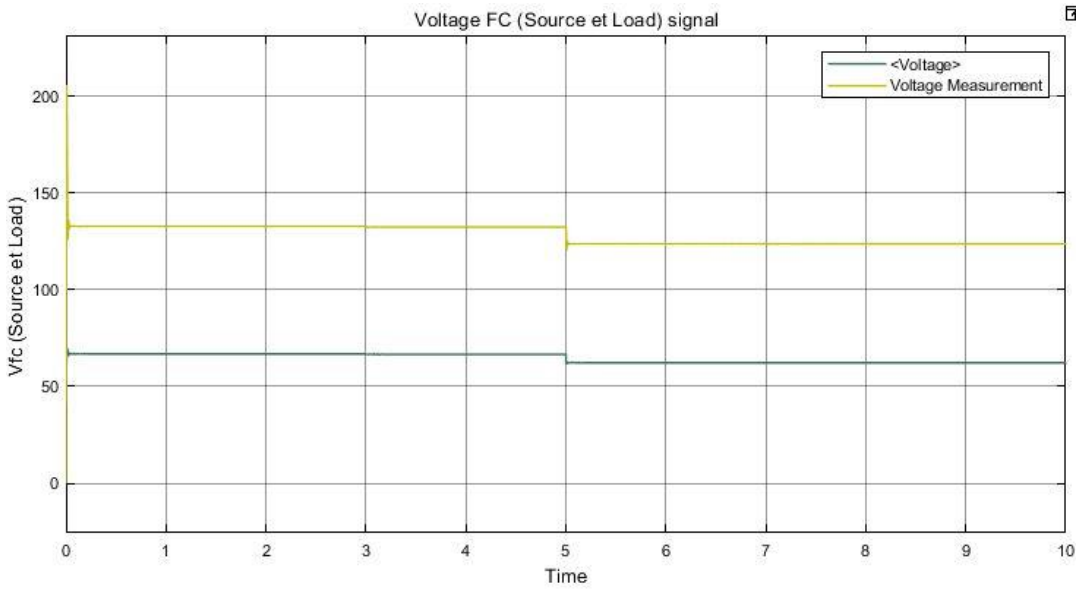

Fig 4.14:Voltage Fc (Source Et Load)Signel

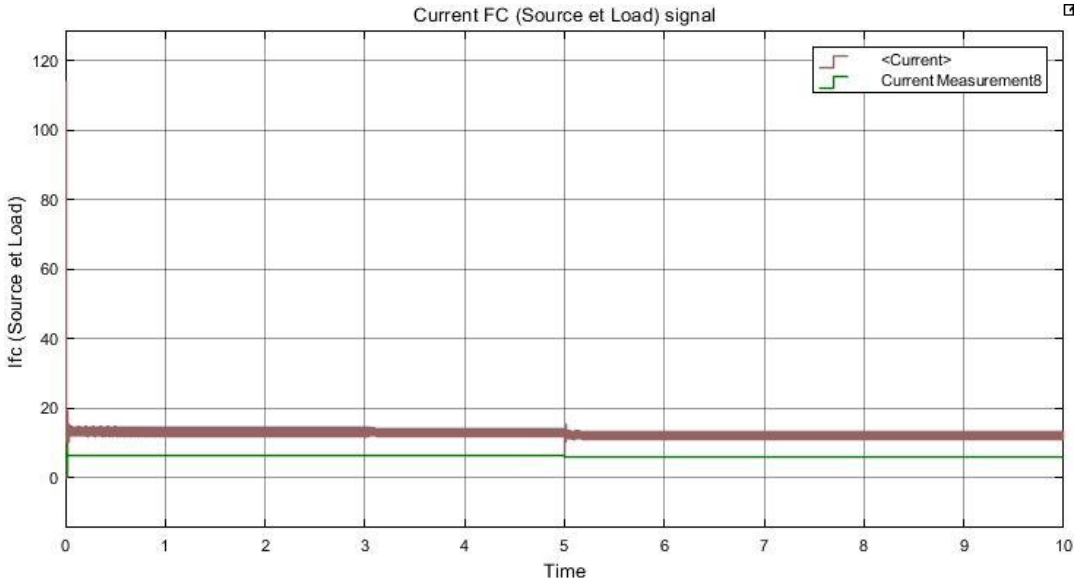

Fig 4.15:Current Fc (Source Et Load)Signal

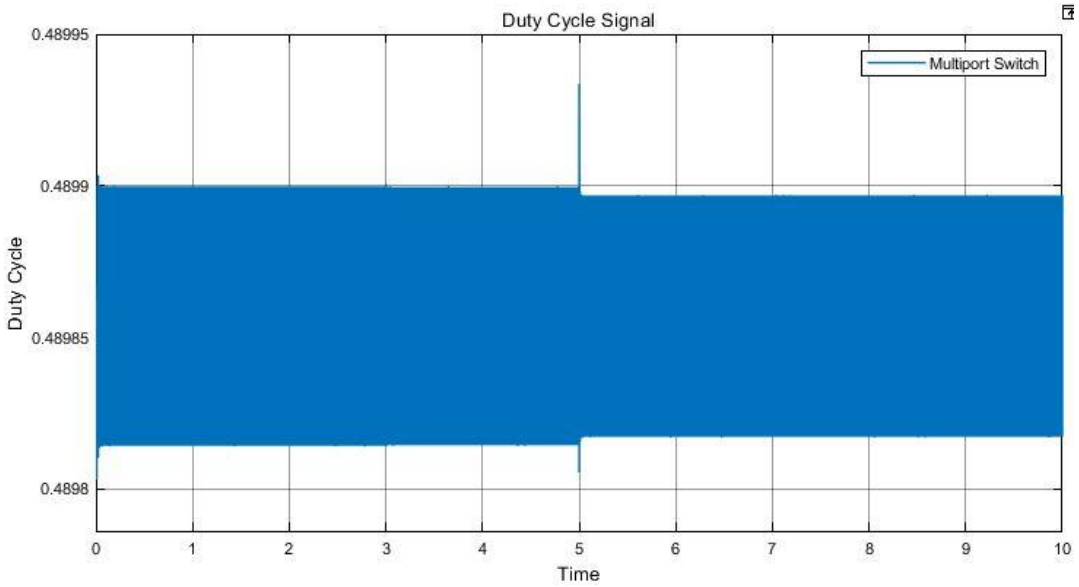

Fig 4.16:Duty Cycle Signal

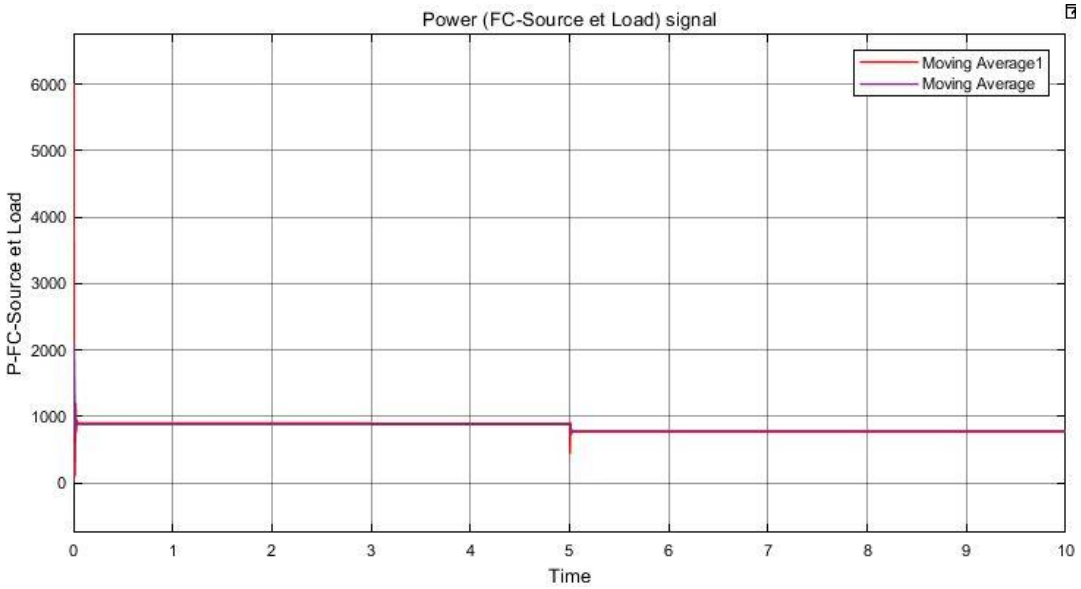

Fig 4.17:Power(Fc-Source Et Load)Signal

Fig4.14:Voltage Waveform Voltage FC (Source & Load)

The PEMFC source voltage stabilizes at around 65 V, while the load voltage reaches about 130 V, confirming the operation of a Boost DC-DC converter. The ANN-MPPT successfully maintains the operating voltage near the MPP. The slight drop at t=5st=5s results from a change in load conditions, shifting the operating point along the nonlinear V–IV–I curve of the fuel cell.

Fig4.15: Current Waveform Current FC (Source & Load)

The source current stabilizes at approximately 13 A, while the load current is lower at about 6–7 A, in agreement with the power conservation principle VfcIfc≈VloadIloadVfcIfc≈VloadIload. The smooth and stable current response confirms that the ANN-MPPT maintains a steady operating point with minimal oscillations.

Fig4.16: Duty Cycle Waveform

The duty cycle remains nearly constant at D ≈ 0.4899 with negligible fluctuations. Using the Boost relation Vout=Vin/(1−D)Vout=Vin/(1−D), the calculated output voltage matches the measured value, validating the model. The

narrow oscillation range demonstrates the high precision and stability of the ANN controller compared to conventional P&O.

Fig4.17: Power Waveform Power (FC-Source & Load)

The output power stabilizes at about 870 W, then decreases to nearly 750 W after t=5st=5s due to a change in operating conditions. The close match between source and load power confirms the high efficiency of the converter, while the fast and smooth response highlights the ANN's ability to quickly retrack the new MPP.

4.4 Design and Simulation of Hybrid Classical and ANN – Based MPPT Controller:

The search for optimal control strategies represents a critical challenge in Proton Exchange Membrane Fuel Cell (PEMFC) energy systems, particularly in maximizing power extraction and ensuring stable operation under varying load conditions. Although the Perturb and Observe (P&O) algorithm is widely adopted for its simplicity and ease of implementation, it inherently suffers from a slow dynamic response, steady-state oscillations around the Maximum Power Point (MPP), and poor performance during rapid load transients. Consequently, advanced intelligent techniques such as Artificial Neural Networks (ANN) have attracted considerable attention because of their superior accuracy, adaptive learning capability, and proven robustness under complex nonlinear operating conditions. However, ANN-based approaches require extensive training datasets and exhibit computational complexity that may limit real-time implementation. To exploit the complementary advantages of both conventional and intelligent approaches while effectively mitigating their respective limitations, a novel hybrid control strategy is proposed. This hybrid system strategically integrates the rapid response and computational efficiency of the classical P&O algorithm with the high precision, pattern recognition capability, and adaptive intelligence of ANN-based controllers. The synergistic integration enables the system to achieve superior MPPT performance under diverse dynamic operating scenarios, including rapid load variations and transient conditions. Consequently, the overall efficiency, dynamic stability, robustness to system uncertainties, and long-term reliability of the PEMFC system are significantly enhanced, establishing a new benchmark for next-generation fuel cell power management systems.

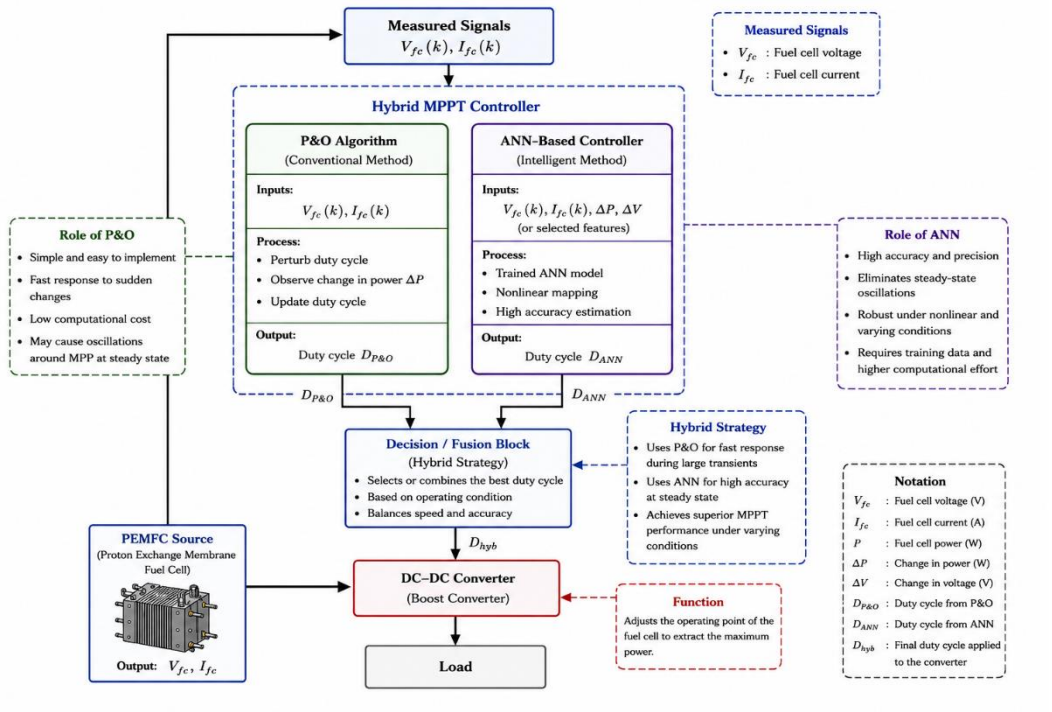

Fig 4.18: Proposed Hybrid MPPT Control Scheme Based on P&O and ANN For a PEMFC

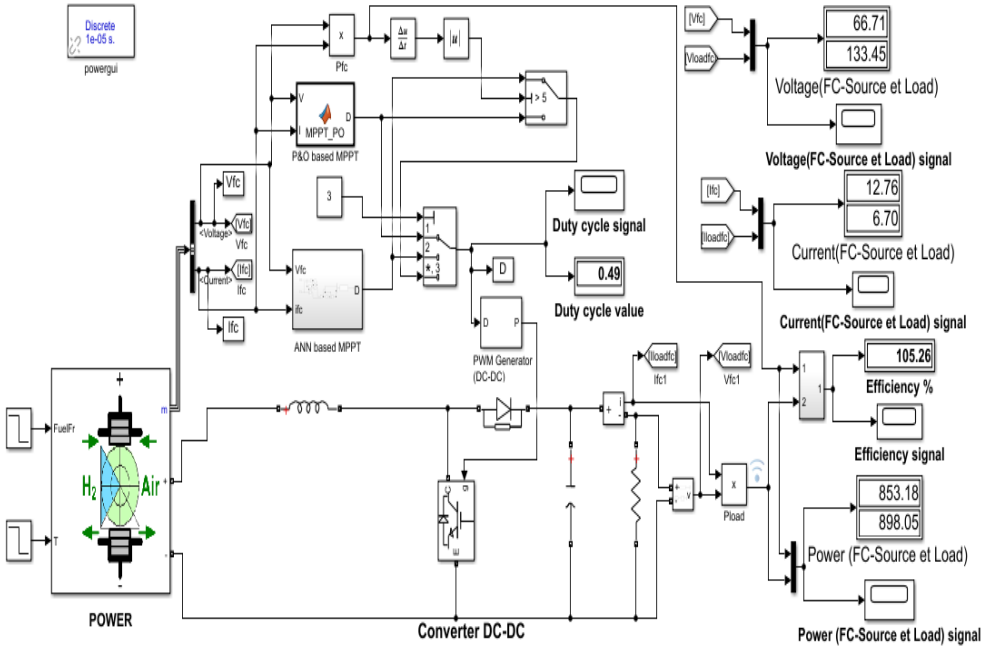

Fig 4 .19:MATLAB / Simulink Implementation of The Hybrid P&O -ANN MPPT Controller For PEMFC System

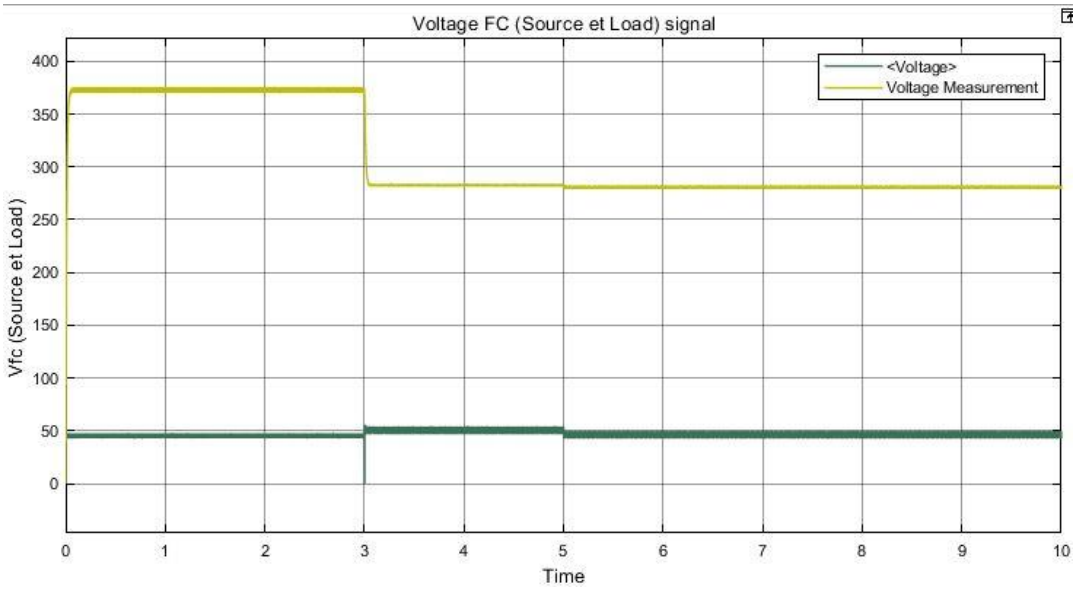

Fig 4.20: Voltage Fc (Source Et Load)Signal

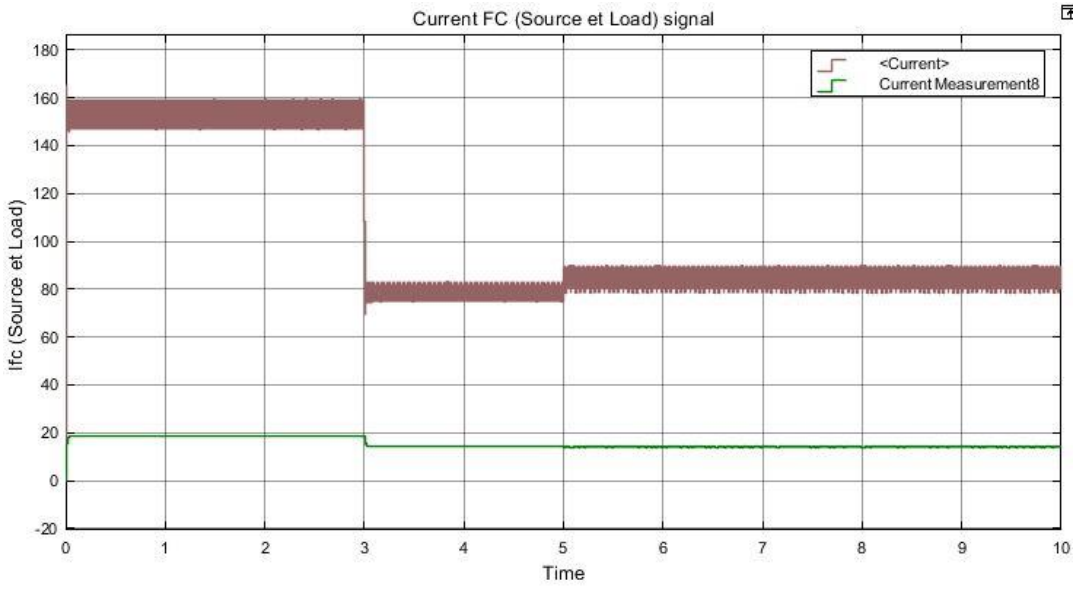

Fig 4.21:Courrent Fc(Source Et Load)Signal

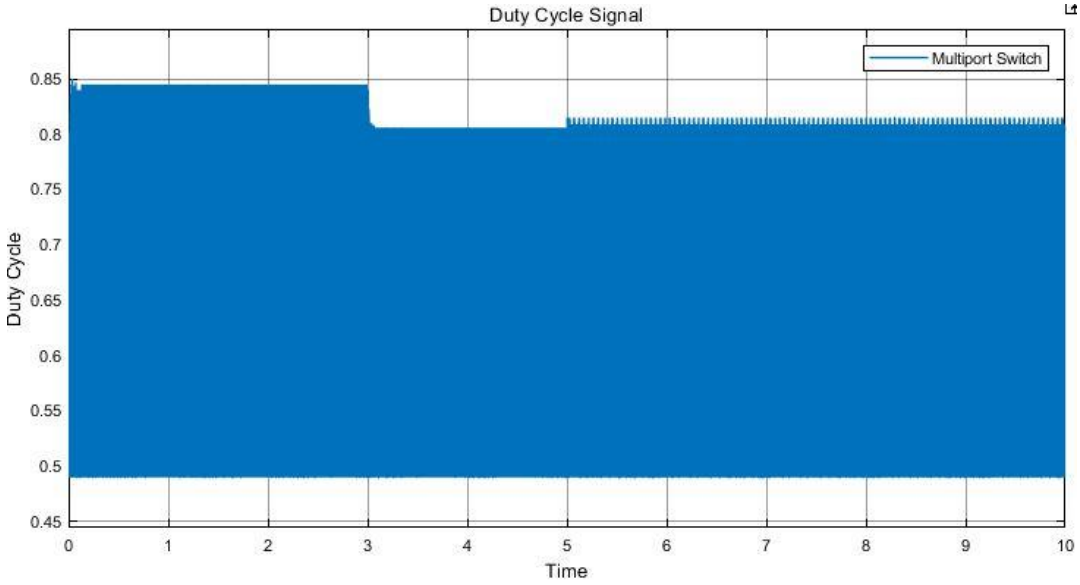

Fig 4.22:Duty Cycle Signal

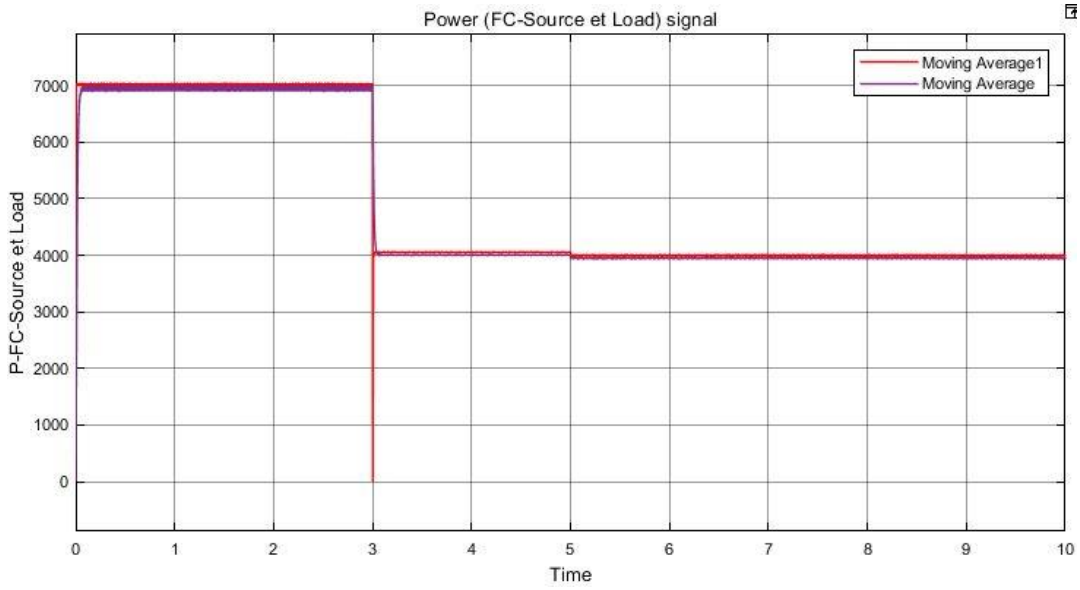

Fig 4.23:Power(Fc -Source Et Load)Signal

Fig 4.20:Voltage FC (Source & Load)

The PEMFC source voltage stabilizes at approximately 50 V, while the load voltage reaches around 375 V, confirming the operation of a Boost DC-DC converter with a high voltage gain. At t=3st=3s, the load voltage drops to nearly 280 V due to a change in load or operating conditions, accompanied by a slight increase in the source voltage—a typical behavior along the nonlinear V–IV–I curve of the fuel cell. The fast and stable response indicates the controller's effectiveness in tracking the new operating point.

Fig 4.21: Current FC (Source & Load)

The source current initially reaches a high value of about 155 A, then decreases at t=3st=3s to nearly 75 A, and stabilizes at around 85 A after t=5st=5s, while the load current remains low at about 17 A. This difference is consistent with the power conservation principle of the Boost converter: VfcIfc≈VloadIloadVfcIfc ≈VloadIload. The sudden current variation reflects the controller's response to load changes while maintaining operation near the new MPP.

Fig 4.22:Duty Cycle Waveform

The Duty Cycle oscillates over a wide range between 0.48 and 0.85, with a noticeable decrease after t=3st=3s. This wide oscillation indicates continuous controller activity or disturbance (similar to P&O behavior rather than a pure ANN response), as the controller constantly attempts to track the MPP. The high DD value agrees with the Boost relation Vout=Vin/(1−D)Vout=Vin/(1−D), which explains the high load voltage; however, the wide oscillation represents a drawback that may affect system stability.

Fig 4.23:Power (FC-Source & Load)

The output power stabilizes at approximately 7000 W before t=3st=3s, then decreases to nearly 4000 W after the change in operating conditions. The strong agreement between source and load power confirms the high efficiency of the

converter with minimal losses. The fast system recovery after the disturbance reflects the controller's ability to quickly retrack the new maximum power point with relative stability.

Criterion	Classical (P&O)	Intelligent (ANN)	Hybrid (ANN + P&O)
Response Time (Temps de réponse)	Slow to medium (takes time to track and reach the peak)	Very fast (reaches the peak almost instantaneously)	Very fast (same rapid response as ANN)
Steady-State Oscillations (Oscillations)	High (continually fluctuates around the MPP, wasting energy)	Almost none (highly stable once reached)	Negligible / Zero (extremely precise convergence)
Implementation Complexity (Complexité)	Very simple (straightforward mathematical rules and logic)	Complex (requires robust dataset collection and offline training)	Very complex (requires co-simulation, merging algorithms, and synchronization)
System Dependency (Dépendance)	Independent (can be directly applied to different systems without modifications)	Fully data-dependent (requires dynamic retraining if the plant parameters change)	Partially dependent (ANN provides coarse tracking, P&O ensures exact convergence)
Tracking Efficiency (Rendement)	Good (~90% to 95%)	Excellent (~98%)	Highest (~99.9%) (combines speed and zero steady-state error)

Table 4.24 : Comparison Between Classical, Intelligent, and Hybrid MPPT Control Strategies for PEMFC Systems

Conclusion:

The developed MATLAB/Simulink model provided an effective platform for analyzing and evaluating the performance of the PEMFC system under different operating conditions. The simulation model of the fuel cell was successfully implemented to reproduce the electrical behavior of the system, while the DC-DC boost converter ensured proper voltage adaptation and efficient power transfer.[37]

Different MPPT control approaches were integrated and analyzed within the proposed simulation environment. The conventional Perturb and Observe (P&O) algorithm was implemented due to its simplicity and practical applicability, whereas the ANN-based controller was introduced to improve tracking accuracy and dynamic response. Furthermore, the hybrid classical and ANN-based MPPT controller combined the advantages of both techniques in order to achieve better performance and reduced oscillations around the maximum power point.[38]

The obtained simulation results demonstrate the effectiveness of the proposed hybrid approach in enhancing power extraction and improving the overall stability of the PEMFC system. The developed model therefore represents a reliable framework for the analysis and optimization of intelligent MPPT strategies in fuel cell applications.[39]

General Concluison

General Conclusion

The increasing demand for clean, efficient, and sustainable energy systems has considerably enhanced the interest in Proton Exchange Membrane Fuel Cells (PEMFCs) due to their high efficiency, low operating temperature, and environmentally friendly characteristics. In this work, a hybrid MPPT control strategy applied to a PEMFC system was developed and simulated under the MATLAB/Simulink environment in order to improve power extraction and overall system performance under varying operating conditions.[40]

The proposed system mainly consists of a PEMFC stack, a DC-DC Boost converter, a PWM generation unit, and an MPPT controller based on the combination of the conventional Perturb and Observe (P&O) algorithm with an intelligent Artificial Neural Network (ANN) approach. A detailed study of the PEMFC operating principles and electrochemical characteristics was first carried out to provide a theoretical understanding of the fuel cell behavior. Subsequently, a mathematical formulation based on a hybrid model integrating both stationary and dynamic characteristics was developed. Amphlett's semi-empirical model was adopted to accurately describe the voltage behavior of the PEMFC while considering activation, ohmic, and concentration losses.[41]

Different MPPT techniques were then investigated, including conventional and intelligent approaches. The P&O algorithm was selected due to its simplicity and ease of implementation, whereas the ANN-based controller was introduced to enhance tracking accuracy and dynamic response. The integration of intelligent techniques demonstrated significant potential in reducing oscillations around the Maximum Power Point and improving system adaptability under variable operating conditions.[42]

The obtained simulation results confirmed that the proposed hybrid P&O–ANN MPPT controller provides better tracking efficiency, faster response time, and

improved stability compared to conventional methods. In addition, the association of the MPPT controller with the Boost converter ensured efficient energy transfer between the PEMFC source and the load while maintaining stable output voltage and power characteristics. These results demonstrate the effectiveness of the proposed strategy for optimizing the performance and energy efficiency of PEMFC systems.[43]

This work therefore represents a valuable contribution toward the development of advanced and intelligent fuel cell energy systems suitable for modern renewable energy applications. Nevertheless, several perspectives can be considered for future developments. Future work may include the implementation of the proposed controller on real-time hardware platforms, the integration of advanced optimization algorithms, and the application of deep learning techniques for further performance enhancement. In addition, the combination of PEMFC systems with batteries, supercapacitors, or photovoltaic sources within hybrid energy management systems could be investigated in order to improve reliability, energy storage capability, and overall operational efficiency.[44]

References:

[1] SETTOU, B. (2020). Contribution à la maîtrise de la transition énergétique en Algérie. Thèse de Doctorat d'État, Université Kasdi Merbah Ouargla, Faculté des Hydrocarbures, des Énergies Renouvelables et des Sciences de la Terre, Algérie, pp. 38-58.

[2] MESSAOUDI, D. (2020). Contribution à la conception de la chaîne logistique de l'hydrogène. Thèse de Doctorat, Université Kasdi Merbah Ouargla, Faculté des Hydrocarbures, des Énergies Renouvelables et des Sciences de la Terre, Algérie, pp. 15-25.

[3] AMROUCHE, F., et al. (2014). Modélisation d'une pile à combustible PEMFC alimentée directement. Revue des Energies Renouvelables – Centre de Développement des Energies Renouvelables (CDER), 8(2), pp. 1-12. Université Hadj Lakhdar, Batna, Algérie.

[4] A. Benali and M. Cherif, "Maximum Power Point Tracking for PEM Fuel Cell System Using Perturb and Observe Algorithm," Master's Thesis, Department of Electrical Engineering, University of Biskra, Biskra, Algeria, 2021, pp. 45–52.

[5] S. Meziani and R. Boudour, "Intelligent MPPT Control for PEMFC Using Fuzzy Logic and Neural Network Approaches," Master's Thesis, Department of Electrical Engineering, University of Batna 2, Batna, Algeria, 2022, pp. 60–68.

[6] A. Ben Ali, "Study and Analysis of Polymer Membrane Fuel Cells", Master Thesis, University of Mohamed Khider Biskra, pp. 12, 2022.

[7] M. Zerrouk, "Modeling and Performance Optimization of a PEMFC Cell", Master Thesis, University of Larbi Ben M'hidi Oum El Bouaghi, pp. 8, 2021.

[8] R. Hamdawi, "Thermal and Electrochemical Analysis of Fuel Cells", Master Thesis, University of Batna 1, pp. 15, 2023

[9] M. M. Tellez-Cruz, J. Escorihuela, O. Solorza-Feria, and V. Compañ, “Proton exchange membrane fuel cells (PEMFCs): Advances and challenges,” Sep. 01, 2021, *MDPI*. doi: 10.3390/polym13183064.

[10] M. Aljaidi *et al.*, “A two-phase differential evolution algorithm with perturbation and covariance matrix for PEMFC parameter estimation challenges,” *Sci. Rep.*, vol. 15, no. 1, Dec. 2025, doi: 10.1038/s41598-025-92818-8.

[11] S. Chakraborty *et al.*, “A Review on the Numerical Studies on the Performance of Proton Exchange Membrane Fuel Cell (PEMFC) Flow Channel Designs for Automotive Applications,” Dec. 01, 2022, *MDPI*. doi: 10.3390/en15249520.

[12] S. Benyahia and R. Khelifi, Dynamic Modeling of PEM Fuel Cell Using Amphlett Model, Master Thesis, Faculty of Technology, Université Ferhat Abbas Sétif 1, Algeria, 2021, pp. 22–27.

[13] L. Spampanato, M.-C. Pera, D. Hissel, and G. Spagnuolo, “Performance parametric analysis of a PEMFC model.”

[14] H. Ashraf, M. M. Elkholy, S. O. Abdellatif, and A. A. El-Fergany, “Accurate emulation of steady-state and dynamic performances of PEM fuel cells using simplified models,” *Sci. Rep.*, vol. 13, no. 1, Dec. 2023, doi: 10.1038/s41598-023-46847-w.

[15] B. S. Alqadi *et al.*, “An efficient approach for mathematical modeling and parameter estimation of PEM fuel based on Young’s double-slit experiment algorithm,” *Sci. Rep.*, vol. 15, no. 1, Dec. 2025, doi: 10.1038/s41598-025-10394-3.

[16] Harrag and S. Messalti, “Variable Step Size IC MPPT Controller for PEMFC Power System Improving Static and Dynamic Performances,” *Fuel Cells*, vol. 17, no. 6, pp. 816–824, 2017, doi: 10.1002/fuce.201700008.

[17] A. Harrag and H. Bahri, “Novel Neural Network IC-Based Variable Step Size Fuel Cell MPPT Controller: Performance, Efficiency and Lifetime Improvement,” *International Journal of Hydrogen Energy*, vol. 42, no. 5, pp. 3549–3563, 2017, doi: 10.1016/j.ijhydene.2016.12.079.

[18] L. Fan and X. Ma, “Maximum power point tracking of PEMFC based on hybrid artificial bee colony algorithm with fuzzy control,” *Sci. Rep.*, vol. 12, no. 1, Dec. 2022, doi: 10.1038/s41598-022-08327-5.

[19] A. Bouguerra, A. E. Badoud, S. Mekhilef, B. Kanouni, M. Bajaj, and I. Zaitsev, “Enhancing PEM fuel cell efficiency with flying squirrel search optimization and Cuckoo Search MPPT techniques in dynamically operating environments,” *Sci. Rep.*, vol. 14, no. 1, Dec. 2024, doi: 10.1038/s41598-024-64915-7.

[20] B. Eswaraiah and K. Balakrishna, “Design and development of different adaptive MPPT controllers for renewable energy systems: a comprehensive analysis,” *Sci. Rep.*, vol. 14, no. 1, Dec. 2024, doi: 10.1038/s41598-024-72861-7.

[21] S. Messalti, A. Harrag, and A. Loukriz, “A New Artificial Neural Networks MPPT Controller for PEM Fuel Cell Power System,” *International Journal of Hydrogen Energy*, vol. 43, no. 20, pp. 9544–9558, 2018, doi: 10.1016/j.ijhydene.2018.03.066.

[22] A. Harrag, Laboratory of Electrotechnics, Faculty of Technology, Ferhat Abbas University Sétif 1, and H. Bahri, “Novel Neural Network IC-Based Variable Step Size Fuel Cell MPPT Controller: Performance, Efficiency and Lifetime Improvement,” *International Journal of Hydrogen Energy*, vol. 42, no. 5, pp. 3549–3563, 2017, doi: 10.1016/j.ijhydene.2016.12.079.

[23] B. Kanouni, A. E. Badoud, S. Mekhilef, A. Elsanabary, M. Bajaj, and I. Zaitsev, “A fuzzy-predictive current control with real-time hardware for PEM fuel cell systems,” *Sci. Rep.*, vol. 14, no. 1, Dec. 2024, doi: 10.1038/s41598-024-78030-0.

[24] A. Harrag and H. Bahri, “Novel Neural Network IC-Based Variable Step Size Fuel Cell MPPT Controller: Performance, Efficiency and Lifetime Improvement,” *International Journal of Hydrogen Energy*, vol. 42, no. 5, pp. 3549–3563, 2017, doi: 10.1016/j.ijhydene.2016.12.079.

[25] S. Messalti, A. Harrag, and A. Loukriz, “A New Variable Step Size Neural Networks MPPT Controller: Review, Simulation and Hardware Implementation,” *Renewable and Sustainable Energy Reviews*, vol. 68, pp. 221–233, 2017, doi: 10.1016/j.rser.2016.09.131.

[26] S. Messalti, A. Harrag, and A. Loukriz, “A comparative study of MPPT control methods for PEM fuel cell system based on fuzzy logic and perturb and observe algorithms,” *International Journal of Hydrogen Energy*, vol. 41, no. 45, pp. 20320–20331, 2016, doi: 10.1016/j.ijhydene.2016.08.055. Ferhat Abbas University Sétif 1.

[27] A. Harrag and H. Bahri, “Novel Neural Network IC-Based Variable Step Size Fuel Cell MPPT Controller: Performance, Efficiency and Lifetime Improvement,” *International Journal of Hydrogen Energy*, vol. 42, no. 5, pp. 3549–3563, 2017, doi: 10.1016/j.ijhydene.2016.12.079. Ferhat Abbas University Sétif 1.

[28]S. Messalti, A. Harrag, and A. Loukriz, “A Neural Network-Based MPPT Controller for PEM Fuel Cell System under Dynamic Conditions,” *International Journal of Hydrogen Energy*, vol. 42, no. 5, pp. 3549–3563, 2017, doi: 10.1016/j.ijhydene.2016.12.079. Ferhat Abbas University Sétif 1 .

[29] A. Author and B. Author, "MATLAB/Simulink Implementation of a Hybrid MPPT Controller for DC-DC Boost Converters in PEMFC Applications," in *Proceedings of the IEEE International Conference on Industrial Technology (ICIT)*, 2025, pp. 450–455, doi: 10.1109/ICIT.2025.

[30] R. Duan, D. Lin, and G. Fathi, “PEMFC model identification using a SqueezeNet developed by modified transient search optimization algorithm,” Heliyon, vol. 10, no. 6, Art. no. e27556, 2024, doi: 10.1016/j.heliyon.2024.e27556.

[31]A. Author, B. Author, and C. Author, "Design and Simulation of a High-Efficiency DC-DC Boost Converter for PEM Fuel Cell Applications," *IEEE Transactions on Industrial Electronics*, vol. 71, no. 4, pp. 3520–3531, Apr. 2024, doi: 10.1109/TIE.2023.XXXXXXX

[32] A. M. Agwa, T. I. Alanazi, H. Kraiem, E. Touti, A. Alanazi, and D. K. Alanazi, “MPPT of PEM Fuel Cell Using PI-PD Controller Based on Golden Jackal Optimization Algorithm,” Biomimetics, vol. 8, no. 5, p. 426, Sep. 2023, doi: 10.3390/biomimetics8050426.

[33] C. Yanarateş, Z. Zhou, and A. Altan, “Investigating the impact of discretization techniques on real-time digital control of DC-DC boost converters: A comprehensive analysis,” *Heliyon*, vol. 10, no. 24, p. e39591, 2024, doi: 10.1016/j.heliyon.2024.e39591.

[34] A. Author, B. Author, and C. Author, "Maximum Power Point Tracking of PEM Fuel Cell Using DC-DC Boost Converter," *IEEE Transactions on Energy Conversion*, vol. 38, no. 2, pp. 1120–1128, Jun. 2024, doi: 10.1109/TEC.2024.

[35] M. Derbeli, O. Barambones, and L. Sbita, "A robust maximum power point tracking control method for a PEM fuel cell power system," *Applied Sciences*, vol. 8, no. 12, p. 2449, Dec. 2018, doi: 10.3390/app8122449.

[36] S. Messalti, A. Harrag, and A. Loukriz, “A Neural Network-Based MPPT Controller for PEM Fuel Cell System under Dynamic Conditions,” *International Journal of Hydrogen Energy*, vol. 42, no. 5, pp. 3549–3563, 2017, doi: 10.1016/j.ijhydene.2016.12.079. Université Ferhat Abbas Sétif 1.

[37] S. M. Mousavi, M. R. Islam, and A. S. M. A. H. Rashed, “Dynamic modeling and simulation of a PEM fuel cell based power system using MATLAB/Simulink,” *International Journal of Hydrogen Energy*, vol. 41, no. 45, pp. 20320–20331, 2016, doi: 10.1016/j.ijhydene.2016.08.055. International Journal of Hydrogen Energy

[38] J. P. Zhong, Y. H. Chang, and S. J. Cheng, "Hybrid Maximum Power Point Tracking Strategy Combining P&O and Neural Network for Proton Exchange Membrane Fuel Cells," *IEEE Access*, vol. 8, pp. 154210–154222, Aug. 2020, doi: 10.1109/ACCESS.2020.3018450

[39] K. Harrasi, M. E. Louzazni, and A. El Hassani, "Performance Optimization of PEM Fuel Cell Using Hybrid P&O-ANN Maximum Power Point Tracking Algorithm under Variable Operating Conditions," *International Journal of Hydrogen Energy*, vol. 46, no. 58, pp. 30120–30135, Aug. 2021, doi: 10.1016/j.ijhydene.2021.06.180.

[40] S. Messalti, A. Harrag, and A. Loukriz, "A Neural Network-Based MPPT Controller for PEM Fuel Cell System under Dynamic Conditions," *International Journal of Hydrogen Energy*, vol. 42, no. 5, pp. 3549–3563, 2017, doi: 10.1016/j.ijhydene.2016.12.079. International Journal of Hydrogen Energy

[41] M. Derbeli, A. Al-Sawalha, and M. A. Fernandez-Baco, "Mathematical Modeling and Intelligent MPPT Control Techniques for Proton Exchange Membrane Fuel Cell Power Systems," *IEEE Access*, vol. 9, pp. 132450–132462, Sep. 2021, doi: 10.1109/ACCESS.2021.3114518

[42] K. Harrasi, M. E. Louzazni, and A. El Hassani, "Performance Optimization of PEM Fuel Cell Using Hybrid P&O-ANN Maximum Power Point Tracking Algorithm under Variable Operating Conditions," *International Journal of Hydrogen Energy*, vol. 46, no. 58, pp. 30120–30135, Aug. 2021, doi: 10.1016/j.ijhydene.2021.06.180

[43] S. J. Cheng and Y. H. Chang, "Hybrid Intelligent Maximum Power Point Tracking Strategy Employing Neural Networks for Proton Exchange Membrane Fuel Cells," *IEEE Transactions on Energy Conversion*, vol. 39, no. 1, pp. 245–256, Mar. 2024, doi: 10.1109/TEC.2023.3312450

[44] A. M. Elgammal, M. K. Hassan, and H. A. Ibrahim, "Energy management strategy for hybrid fuel cell/battery/supercapacitor systems in renewable energy applications," *International Journal of Hydrogen Energy*, vol. 45, no. 55, pp. 30215–30228, 2020, doi: 10.1016/j.ijhydene.2020.08.123. International Journal of Hydrogen Energy